arXiv:hep-ph/9803428v2 27 Mar 1998

DESY 98-030
March 1998

Perturbative QCD- and Power-Corrected Hadron Spectra and Spectral Moments in the Decay $B \to X_s \ell^+ \ell^-$

A. Ali[*] **and G. Hiller**[†]
Deutsches Elektronen-Synchrotron DESY, Hamburg

Abstract

We compute the leading order (in α_s) perturbative QCD and power ($1/m_b^2$) corrections to the hadronic invariant mass and hadron energy spectra in the decay $B \to X_s \ell^+ \ell^-$ in standard model. The computations are carried out using the heavy quark expansion technique (HQET) and a perturbative-QCD improved Fermi motion (FM) model which takes into account B-meson wave-function effects. The corrections in the hadron energy (E_H) spectrum are found to be small over a good part of this spectrum in both methods. However, the expansion in $1/m_b$ in HQET fails near the lower kinematic end-point and at the $c\bar{c}$ threshold. The hadronic invariant mass (S_H) spectrum is calculable only over a limited range $S_H > \bar{\Lambda} m_B$ in the heavy quark expansion, where $\bar{\Lambda} \simeq m_B - m_b$. We also present results for the first two hadronic moments $\langle S_H^n \rangle$ and $\langle E_H^n \rangle$, $n = 1, 2$, working out their sensitivity on the HQET and FM model parameters. For equivalent values of these parameters, the moments in these methods are remarkably close to each other. The constraints following from assumed values of $\langle S_H^n \rangle$ on the HQET parameters λ_1 and $\bar{\Lambda}$ are worked out. Data from the forthcoming B facilities could be used to measure the short-distance contribution in $B \to X_s \ell^+ \ell^-$and constrain the HQET parameters λ_1 and $\bar{\Lambda}$. This could be combined with complementary constraints from the decay $B \to X \ell \nu_\ell$ to determine these parameters precisely. We also study the effect of the experimental cuts, used recently by the CLEO collaboration in searching for the decay $B \to X_s \ell^+ \ell^-$, on the branching ratios, hadron spectra and hadronic invariant mass moments using the FM model.

(Submitted to Physical Review D)

---

[*] E-mail address: ali@x4u2.desy.de
[†] E-mail address: ghiller@x4u2.desy.de

1 Introduction

The semileptonic inclusive decays $B \to X_s \ell^+ \ell^-$, where $\ell^\pm = e^\pm, \mu^\pm, \tau^\pm$, offer, together with the radiative electromagnetic penguin decay $B \to X_s + \gamma$, presently the most popular testing grounds for the standard model (SM) in the flavor sector. This is reflected by the impressive experimental and theoretical activity in this field, reviewed recently in [1] and [2], respectively. We shall concentrate here on the decay $B \to X_s \ell^+ \ell^-$ for which the first theoretical calculations were reported a decade ago [3–5], emphasizing the sensitivity of the dilepton mass spectrum and decay rate to the top quark mass in the short-distance contribution. With the discovery of the top quark and a fairly accurate measurement of its mass [6], theoretical emphasis has changed from predicting the top quark mass using this decay to using its measured value as input and making theoretically accurate predictions for the decay rates and spectra. This will help confront the predictions in the SM with experiment more precisely and will allow to search for new phenomena, such as supersymmetry [7–11].

Since these early papers, considerable theoretical work has been done on the decay $B \to X_s \ell^+ \ell^-$ in the context of the standard model. This includes, among other aspects, the calculation of the complete leading order perturbative corrections in the QCD coupling constant α_s to the dilepton invariant mass spectrum [12,13], forward-backward (FB) asymmetry of the leptons [14,15], and, additionally, leading order power corrections in $1/m_b^2$ to the decay rate, dilepton invariant mass spectrum and FB asymmetry [15], using the heavy quark expansion technique (HQET) [16–18]. We recall that the $1/m_b^2$ corrections to the dilepton spectrum and decay rate in $B \to X_s \ell^+ \ell^-$were calculated in ref. [18] but their results were at variance with the ones derived later in ref. [15]. The power corrected dilepton mass spectrum and FB asymmetry have been rederived for the massless s-quark case recently [19], confirming the results in ref. [15]. Corrections of order $1/m_c^2$ to the dilepton mass spectrum away from the $(J/\psi, \psi', ...)$-resonant regions have also been worked out [20,21], making use of earlier work on similar power corrections in the decay rate for $B \to X_s + \gamma$ [22,23]. The $1/m_b^2$ power corrections to the left-right asymmetry [24,25] have been presented in [19] correcting an earlier calculation of the same [25]. Likewise, the longitudinal polarization of the lepton, P_L, in $B \to X_s \tau^+ \tau^-$ at the partonic level has been worked out [26]; the other two orthogonal polarization components P_T (the component in the decay plane) and P_L (the component normal to the decay plane) were subsequently worked out in ref. [27]. As an alternative to HQET, B-meson wave-function effects in the decay $B \to X_s \ell^+ \ell^-$ have also been studied for the dilepton invariant mass spectrum and FB asymmetry [15], using the Fermi motion (FM) model [28]. Some of the cited works have also addressed the long-distance aspect of the decay $B \to X_s \ell^+ \ell^-$having to do with the resonant structure of the dilepton invariant mass spectrum. We shall leave out the $J/\psi, \psi', ...$-resonant contributions in this paper and will present a detailed phenomenological study including them elsewhere [29].

This theoretical work, despite some uncertainties associated with the LD-part, will undoubtedly contribute significantly to a meaningful comparison of the SM and experiment in the decay $B \to X_s \ell^+ \ell^-$. Still, concerning the SD-contribution, some aspects of this decay remain to be studied theoretically. In the context of experimental searches for $B \to X_s \ell^+ \ell^-$, it has been emphasized (see, for example, the CLEO paper [30]) that theoretical estimates of the hadronic invariant mass and hadron energy spectra in this decay will greatly help in providing improved control of the signal and they will also be needed to correct for the experimental acceptance. In addition to their experimental utility, hadron spectra in heavy hadron decays are also of considerable theoretical interest in their own right, as reflected by similar studies done for the charged current induced semileptonic decays $B \to X_c \ell \nu_\ell$ and $B \to X_u \ell \nu_\ell$ [31–35], where the main emphasis has been on testing HQET and/or in determining the Cabibbo-Kobayashi-Maskawa (CKM) matrix elements V_{cb} and V_{ub}. The hadronic invariant mass spectra in $b \to s \ell^+ \ell^-$ and $b \to u \ell^- \nu_\ell$ decays have striking similarities and differences. For example, both of these processes have at the parton level a delta function behavior $d\Gamma/ds_0 \propto \delta(s_0 - m_q^2)$, $q = u, s$, where s_0 is the hadronic invariant mass at the parton level. Thus, the entire invariant mass spectrum away from $s_0 = m_q^2$ is generated perturbatively (by gluon bremsstrahlung) and through the B-hadron non-perturbative effects. Hence, measurements of these spectra would lead to direct information on the QCD dynamics and to a better determination of the non-perturbative parameters. There are also obvious differences in these decays, namely the decay $B \to X_u \ell \nu_\ell$ is intrinsically a lot simpler due to the absence of the resonating $c\bar{c}$ contributions, which one must include to get the inclusive spectra in $B \to X_s \ell^+ \ell^-$, or else use data in restricted phase space where the $c\bar{c}$-resonant contributions are subleading.

Having stated the motivations, we study hadron spectra in the decay $B \to X_s \ell^+ \ell^-$ in this paper. We first compute the leading order (in α_s) perturbative QCD and power $(1/m_b^2)$ corrections to the hadronic invariant mass and hadron energy spectra at the parton level. In addition to the bremsstrahlung contribution $b \to (s + g) \ell^+ \ell^-$, there are important non-perturbative effects even in $\mathcal{O}(\alpha_s^0)$ that come from the relations between the b quark mass and the B meson mass. In HQET, this takes the form $m_B = m_b + \bar{\Lambda} - (\lambda_1 + 3\lambda_2)/2m_b + ...$, where $\bar{\Lambda}$, λ_1 and λ_2 are the HQET parameters [16–18]. Keeping, for the sake of simplicity just the $\bar{\Lambda}$ term, the hadronic invariant mass S_H is related to s_0 and the partonic energy E_0 by $S_H = s_0 + 2\bar{\Lambda} E_0 + \bar{\Lambda}^2$. This gives rise to a non-trivial spectrum in the entire region $\bar{\Lambda}^2 < S_H < M_B^2$. Including both the $\mathcal{O}(1/m_b^2)$ and $\mathcal{O}(\alpha_s)$ terms generates hadron energy and hadronic invariant mas spectrum with terms of $\mathcal{O}(\bar{\Lambda}/m_B)$, $\mathcal{O}(\alpha_s \bar{\Lambda}/m_B)$, $\mathcal{O}(\lambda_1/m_B^2)$ and $\mathcal{O}(\lambda_2/m_B^2)$. The power- and perturbatively corrected hadron spectra up to and including these terms are presented here. The $1/m_b^2$ corrections in the hadron energy spectrum are found to be small over a good part of this spectrum. However, the expansion in $1/m_b$ fails near the lower end-point and near the $c\bar{c}$ threshold. The hadronic invariant mass spectrum is reliably calculable over a limited region only, namely for $S_H > \bar{\Lambda} m_B$. Hadronic moments $\langle S_H^n \rangle$ and $\langle E_H^n \rangle$, on the other hand, are calculable in HQET and we have summarized the results for the first two moments $n = 1, 2$ in a letter [36], based on this study. The hadronic invariant mass moments are sensitive to the HQET parameters $\bar{\Lambda}$ and λ_1. This provides potentially an independent determination of these quantities. We think that the hadron spectra in $B \to X_s \ell^+ \ell^-$and $B \to X_u \ell \nu_\ell$ can be related to each other over limited phase space and this could help in vastly improving the present precision on V_{ub} [6] and the parameters λ_1 and $\bar{\Lambda}$ [37,38].

In view of the continued phenomenological interest in the FM model [28], motivated in part by its close resemblance to the HQET framework [39,17], we also compute the hadron spectra in $B \to X_s \ell^+ \ell^-$ in this model, taking into account the $\mathcal{O}(\alpha_s)$ perturbative QCD corrections. The FM model is characterized by two parameters which are usually taken as p_F, the Gaussian width of the b-quark momentum, and m_q, the spectator quark mass in the B hadron; the b-quark mass is a momentum-dependent quantity (see section 6 for details). The matrix element of the kinetic energy operator, λ_1 and the binding energy $\bar{\Lambda}$ can be calculated in terms of the FM model parameters. The difference between the effective b-quark mass, which is a derived quantity in the FM model, and the B-meson mass can also be expressed via an HQET-type relation, $m_B = m_b^{\rm eff} + \bar{\Lambda} - \lambda_1 / 2 m_b^{\rm eff}$. However, there is no analog of λ_2 in the FM model. Having defined the equivalence between the FM model and HQET parameters, we shall use $\bar{\Lambda}$ and λ_1 to also characterize the FM model parameters. The dependence of the hadron spectra in the FM model in the decay $B \to X_s \ell^+ \ell^-$ on the parameters $\bar{\Lambda}$ and λ_1 is studied in this paper. We find that the hadron energy spectrum in $B \to X_s \ell^+ \ell^-$in the FM model is stable against variations of the model parameters. The hadron energy spectra in the FM model and HQET are also found to be close to each other in regions where HQET holds. This feature was also noticed in the context of the decay $B \to X_u \ell \nu_\ell$ in ref. [33]. The hadronic invariant mass spectrum depends sensitively on the parameters of the FM model - a behavior which has again its parallel in studies related to the decay $B \to X_u \ell \nu_\ell$ [34] as well as in HQET. Hadronic moments $\langle S_H^n \rangle$ and $\langle E_H^n \rangle$ are computed in the FM model and are found to be remarkably close to their counterparts calculated in HQET for equivalent values of the parameters $\bar{\Lambda}$ and λ_1. The picture that emerges from these comparisons is that the spectra and moments in the two approaches are rather similar, though not identical. We also study the effects of the CLEO experimental cuts on the branching ratios, hadron spectra and hadronic moments in $B \to X_s \ell^+ \ell^-$ in the FM model and the results are presented here. These can be compared with data when they become available.

This paper is organized as follows. In section 2, we define the kinematics of the process $B \to X_s \ell^+ \ell^-$ and introduce the quantities of dynamical interest in the framework of an effective Hamiltonian. Leading order (in α_s) perturbative corrections to the hadron energy and hadronic invariant mass spectra at the parton level are derived in section 3, where we also present the Sudakov-improved spectrum $d\mathcal{B}/ds_0$. Using the HQET relation between m_B and m_b, we calculate the corrected hadronic invariant mass spectrum $d\mathcal{B}/dS_H$. In section 4, we present the leading power corrections (in $1/m_b^2$) for the Dalitz distribution $d^2\mathcal{B}/dx_0 d\hat{s}_0$ (here x_0 and $\hat{s}_0$ are the scaled partonic energy and hadronic invariant mass, respectively) and derive analytic expressions for the hadron energy spectrum $d\mathcal{B}/dx_0$ and the resulting spectrum is compared with the one in the parton model. In section 5, we calculate the moments in the hadron energy and hadronic invariant mass in HQET and give the results for $\langle S_H \rangle$, $\langle S_H^2 \rangle$, $\langle E_H \rangle$ and $\langle E_H^2 \rangle$ in terms of the corresponding moments in the partonic variables. Section 6 describes the wave-function effects in the FM model [28] in the hadron energy and hadronic invariant mass spectra. We also give here numerical estimates of the hadronic moments in HQET and the FM model. In section 7, we study the effects of the experimental cuts used in the CLEO analysis of $B \to X_s \ell^+ \ell^-$on the hadron spectra and hadronic moments using the FM model. Estimates of the branching ratios $\mathcal{B}(B \to X_s \ell^+ \ell^-)$ for $\ell = \mu, e$ are also presented here, together with estimates of the survival probability for the CLEO cuts, using the FM model. Section 8 contains a summary of our work and some concluding remarks. Definitions of various auxiliary functions and lengthy expressions appearing in the derivation of our results, including the partonic moments $\langle x_0^n \rangle$, $\langle (\hat{s}_0 - \hat{m}_s)^n \rangle$ and $\langle x_0 (\hat{s}_0 - \hat{m}_s) \rangle$ for $n = 1, 2$ are relegated to the Appendices A - D.

2 The Decay $B \to X_s \ell^+ \ell^-$ in the Effective Hamiltonian Approach

2.1 Kinematics

We start with the definition of the kinematics of the decay at the parton level,

$$b(p_b) \to s(p_s)(+g(p_g)) + \ell^+(p_+) + \ell^-(p_-) \ , \tag{1}$$

where g denotes a gluon from the $O(\alpha_s)$ correction (see Fig. 1). The corresponding kinematics at the hadron level can be written as:

$$B(p_B) \to X_s(p_H) + \ell^+(p_+) + \ell^-(p_-) \ . \tag{2}$$

We define the momentum transfer to the lepton pair and the invariant mass of the dilepton system, respectively, as

$$q \equiv p_+ + p_- \ , \tag{3}$$

$$s \equiv q^2 \ . \tag{4}$$

The dimensionless variables with a hat are related to the dimensionful variables by the scale m_b, the b-quark mass, e.g., $\hat{s} = \frac{s}{m_b^2}$, $\hat{m}_s = \frac{m_s}{m_b}$ etc.. Further, we define a 4-vector v, which denotes the velocity of both the b-quark and the B-meson, $p_b = m_b v$ and $p_B = m_B v$. We shall also need the variable u and the scaled variable $\hat{u} = \frac{u}{m_b^2}$, defined as:

$$\begin{aligned} u &\equiv -(p_b - p_+)^2 + (p_b - p_-)^2 \ , & (5) \\ \hat{u} &= 2v \cdot (\hat{p}_+ - \hat{p}_-) \ . & (6) \end{aligned}$$

The hadronic invariant mass is denoted by $S_H \equiv p_H^2$ and E_H denotes the hadron energy in the final state. The corresponding quantities at parton level are the invariant mass s_0 and the scaled parton energy $x_0 \equiv \frac{E_0}{m_b}$. In parton model without gluon bremsstrahlung, this simplifies to $s_0 = m_s^2$ and x_0 becomes directly related to the dilepton invariant mass $x_0 = 1/2(1 - \hat{s} + \hat{m}_s^2)$. From momentum conservation the following equalities hold in the b-quark, equivalently B-meson, rest frame ($v = (1,0,0,0)$):

$$\begin{aligned} x_0 &= 1 - v \cdot \hat{q} \ , \quad \hat{s}_0 = 1 - 2v \cdot \hat{q} + \hat{s} \ , & (7) \\ E_H &= m_B - v \cdot q \ , \quad S_H = m_B^2 - 2m_B v \cdot q + s \ . & (8) \end{aligned}$$

The relations between the kinematic variables of the parton model and the hadronic states , using the HQET mass relation, can be written as

$$\begin{aligned} E_H &= \bar{\Lambda} - \frac{\lambda_1 + 3\lambda_2}{2m_B} + \left(m_B - \bar{\Lambda} + \frac{\lambda_1 + 3\lambda_2}{2m_B} \right) x_0 + \dots \ , \\ S_H &= m_s^2 + \bar{\Lambda}^2 + (m_B^2 - 2\bar{\Lambda} m_B + \bar{\Lambda}^2 + \lambda_1 + 3\lambda_2)\,(\hat{s}_0 - \hat{m}_s^2) \\ &\qquad + (2\bar{\Lambda} m_B - 2\bar{\Lambda}^2 - \lambda_1 - 3\lambda_2) x_0 + \dots \ , \qquad (9) \end{aligned}$$

where the ellipses denote terms higher order in $1/m_b$.

2.2 Matrix element for the decay $B \to X_s \ell^+ \ell^-$

The effective Hamiltonian obtained by integrating out the top quark and the $W^\pm$ bosons is given as

$$\begin{aligned} \mathcal{H}_{eff}(b \to s + X,\, X = \gamma,\, \ell^+\ell^-) = -\frac{4G_F}{\sqrt{2}} V_{ts}^* V_{tb} \Bigg[\sum_{i=1}^{6} C_i(\mu) O_i + C_7(\mu) \frac{e}{16\pi^2} \bar{s}_\alpha \sigma_{\mu\nu} (m_b R + m_s L) b_\alpha F^{\mu\nu} \\ + C_8(\mu) O_8 + C_9(\mu) \frac{e^2}{16\pi^2} \bar{s}_\alpha \gamma^\mu L b_\alpha \bar{\ell} \gamma_\mu \ell + C_{10} \frac{e^2}{16\pi^2} \bar{s}_\alpha \gamma^\mu L b_\alpha \bar{\ell} \gamma_\mu \gamma_5 \ell \Bigg] \ , (10) \end{aligned}$$

where L and R denote chiral projections, $L(R) = 1/2(1 \mp \gamma_5)$, V_{ij} are the CKM matrix elements and the CKM unitarity has been used in factoring out the product $V_{ts}^* V_{tb}$. The operator basis is taken from [15], where also the Four-Fermi operators $O_1, \dots, O_6$ and the chromo-magnetic operator O_8 can be seen. Note that O_8 does not contribute to the decay $B \to X_s \ell^+ \ell^-$in the approximation which we use here. The $C_i(\mu)$ are the Wilson coefficients, which depend, in general, on the renormalization scale μ, except for C_{10}.

The matrix element for the decay $B \to X_s \ell^+ \ell^-$can be factorized into a leptonic and a hadronic part as

$$\mathcal{M}(B \to X_s \ell^+ \ell^-) = \frac{G_F \alpha}{\sqrt{2}\pi} \, V_{ts}^* V_{tb} \, \left({\Gamma^L}_\mu \, L^{L\mu} + {\Gamma^R}_\mu \, L^{R\mu} \right) , \tag{11}$$

with

$$\begin{aligned} {L^{L/R}}_\mu &\equiv \bar{l} \, \gamma_\mu \, L(R) \, l \, , && (12) \\ {\Gamma^{L/R}}_\mu &\equiv \bar{s} \left[R \, \gamma_\mu \left(C_9^{\rm eff}(\hat{s}) \mp C_{10} + 2 C_7^{\rm eff} \, \frac{\hat{\not{q}}}{\hat{s}} \right) + 2 \hat{m}_s \, C_7^{\rm eff} \, \gamma_\mu \, \frac{\hat{\not{q}}}{\hat{s}} L \right] b \, . && (13) \end{aligned}$$

The effective Wilson coefficient $C_9^{\rm eff}(\hat{s})$ receives contributions from various pieces. The resonant $c\bar{c}$ states also contribute to $C_9^{\rm eff}(\hat{s})$; hence the contribution given below is just the perturbative part:

$$C_9^{\rm eff}(\hat{s}) = C_9 \eta(\hat{s}) + Y(\hat{s}) \, . \tag{14}$$

Here $\eta(\hat{s})$ and $Y(\hat{s})$ represent the $\mathcal{O}(\alpha_s)$ correction [40] and the one loop matrix element of the Four-Fermi operators [12,13], respectively. While C_9 is a renormalization scheme-dependent quantity, this dependence cancels out with the corresponding one in the function $Y(\hat{s})$ (the value of ξ, see below). To be self-contained, we list the two functions in $C_9^{\rm eff}(\hat{s})$:

$$\begin{aligned} Y(\hat{s}) &= g(\hat{m}_c, \hat{s}) \, (3 \, C_1 + C_2 + 3 \, C_3 + C_4 + 3 \, C_5 + C_6) \\ &\quad - \frac{1}{2} g(1, \hat{s}) \, (4 \, C_3 + 4 \, C_4 + 3 \, C_5 + C_6) - \frac{1}{2} g(0, \hat{s}) \, (C_3 + 3 \, C_4) \\ &\quad + \frac{2}{9} \, (3 \, C_3 + C_4 + 3 \, C_5 + C_6) - \xi \, \frac{4}{9} \, (3 \, C_1 + C_2 - C_3 - 3 \, C_4) \, , && (15) \\ \eta(\hat{s}) &= 1 + \frac{\alpha_s(\mu)}{\pi} \omega(\hat{s}) \ , && (16) \end{aligned}$$

$$\xi = \left\{ \begin{array}{ll} 0 & \text{(NDR),} \\ -1 & \text{(HV),} \end{array} \right. \tag{17}$$

$$\begin{aligned} g(z, \hat{s}) &= -\frac{8}{9} \ln(\frac{m_b}{\mu}) - \frac{8}{9} \ln z + \frac{8}{27} + \frac{4}{9} y - \frac{2}{9} (2 + y) \sqrt{|1 - y|} \\ &\quad \times \left[\Theta(1 - y) (\ln \frac{1 + \sqrt{1 - y}}{1 - \sqrt{1 - y}} - i\pi) + \Theta(y - 1) 2 \arctan \frac{1}{\sqrt{y - 1}} \right] \ , && (18) \\ g(0, \hat{s}) &= \frac{8}{27} - \frac{8}{9} \ln(\frac{m_b}{\mu}) - \frac{4}{9} \ln \hat{s} + \frac{4}{9} i\pi \ , && (19) \end{aligned}$$

where $y = 4 z^2 / \hat{s}$, and

$$\begin{aligned} \omega(\hat{s}) &= -\frac{2}{9} \pi^2 - \frac{4}{3} {\rm L}i_2(\hat{s}) - \frac{2}{3} \ln \hat{s} \ln(1 - \hat{s}) - \frac{5 + 4\hat{s}}{3(1 + 2\hat{s})} \ln(1 - \hat{s}) \\ &\quad - \frac{2\hat{s}(1 + \hat{s})(1 - 2\hat{s})}{3(1 - \hat{s})^2 (1 + 2\hat{s})} \ln \hat{s} + \frac{5 + 9\hat{s} - 6\hat{s}^2}{6(1 - \hat{s})(1 + 2\hat{s})} \ . && (20) \end{aligned}$$

Above, (NDR) and (HV) correspond to the naive dimensional regularization and the 't Hooft-Veltman schemes, respectively. The one gluon correction to O_9 with respect to x_0 will be presented below in eq. (26). The Wilson coefficients in leading logarithmic approximation can be seen in [12].

With the help of the above expressions, the differential decay width becomes on using $p_\pm = (E_\pm, \boldsymbol{p}_\pm)$,

$$\mathrm{d}\Gamma = \frac{1}{2m_B} \frac{{G_F}^2\,\alpha^2}{2\pi^2} |V_{ts}^* V_{tb}|^2 \, \frac{\mathrm{d}^3\boldsymbol{p}_+}{(2\pi)^3 2E_+} \frac{\mathrm{d}^3\boldsymbol{p}_-}{(2\pi)^3 2E_-} \left({W^L}_{\mu\nu}\, L^{L\mu\nu} + {W^R}_{\mu\nu}\, L^{R\mu\nu} \right) , \tag{21}$$

where $W^{L,R}_{\mu\nu}$ and $L^{L,R}_{\mu\nu}$ are the hadronic and leptonic tensors, respectively. The hadronic tensor $W^{L/R}_{\mu\nu}$ is related to the discontinuity in the forward scattering amplitude, denoted by $T^{L/R}_{\mu\nu}$, through the relation $W_{\mu\nu} = 2\,\mathrm{Im}\, T_{\mu\nu}$. Transforming the integration variables to $\hat{s}$, $\hat{u}$ and $v \cdot \hat{q}$, one can express the Dalitz distribution in $B \to X_s \ell^+ \ell^-$as:

$$\frac{\mathrm{d}\Gamma}{\mathrm{d}\hat{u}\, \mathrm{d}\hat{s}\, \mathrm{d}(v\cdot\hat{q})} = \frac{1}{2\, m_B} \frac{{G_F}^2\,\alpha^2}{2\,\pi^2} \frac{{m_b}^4}{256\,\pi^4} |V_{ts}^* V_{tb}|^2 \; 2\,\mathrm{Im} \left({T^L}_{\mu\nu}\, L^{L\mu\nu} + {T^R}_{\mu\nu}\, L^{R\mu\nu} \right) , \tag{22}$$

with

$$\begin{aligned} {T^{L/R}}_{\mu\nu} &= i \int \mathrm{d}^4 y\, e^{-i\,\hat{q}\cdot y} \left\langle B \left| \mathrm{T} \left\{ {\Gamma_1}^{L/R}_{\mu}(y), {\Gamma_2}^{L/R}_{\nu}(0) \right\} \right| B \right\rangle , & (23) \\ L^{L/R\mu\nu} &= 2 \left[{p_+}^\mu\, {p_-}^\nu + {p_-}^\mu\, {p_+}^\nu - g^{\mu\nu} (p_+ \cdot p_-) \mp i\epsilon^{\mu\nu\alpha\beta}\, p_{+\alpha}\, p_{-\beta} \right] , & (24) \end{aligned}$$

where ${\Gamma_1}^{L/R^\dagger}_{\mu} = {\Gamma_2}^{L/R}_{\mu} = \Gamma^{L/R}_{\mu}$, and is given in eq. (13). Using Lorentz decomposition, the tensor $T_{\mu\nu}$ can be expanded in terms of three structure functions T_i,

$$T_{\mu\nu} = -T_1\, g_{\mu\nu} + T_2\, v_\mu\, v_\nu + T_3\, i\epsilon_{\mu\nu\alpha\beta}\, v^\alpha\, \hat{q}^\beta , \tag{25}$$

where the structure functions which do not contribute to the amplitude in the limit of massless leptons have been neglected. The problem remaining is now to determine the T_i, to which we shall return in section 4.

3 Perturbative QCD Corrections in $O(\alpha_s)$ in the Decay $B \to X_s \ell^+ \ell^-$

In this section the $O(\alpha_s)$ corrections to the hadron spectra are investigated. Only O_9 is subject to α_s corrections and the renormalization group improved perturbation series for C_9 is $\mathcal{O}(1/\alpha_s) + \mathcal{O}(1) + \mathcal{O}(\alpha_s) + \ldots$, due to the large logarithm in C_9 represented by $\mathcal{O}(1/\alpha_s)$ [12]. The Feynman diagrams, which contribute to the matrix element of O_9 in $O(\alpha_s)$, corresponding to the virtual one-gluon and bremsstrahlung corrections, are shown in Fig. 1. The effect of a finite s-quark mass on the $\mathcal{O}(\alpha_s)$ correction function is found to be very small. After showing this, we have neglected the s-quark mass in the numerical calculations of the $\mathcal{O}(\alpha_s)$ terms.

Parameter	Value
m_W	80.26 (GeV)
m_Z	91.19 (GeV)
$\sin^2\theta_W$	0.2325
m_s	0.2 (GeV)
m_c	1.4 (GeV)
m_b	4.8 (GeV)
m_t	175 ± 5 (GeV)
μ	$m_b{}^{+m_b}_{-m_b/2}$
α^{-1}	129
$\alpha_s(m_Z)$	0.117 ± 0.005
$\mathcal{B}_{sl}$	(10.4 ± 0.4) %

Table 1: *Default values of the input parameters and errors used in the numerical calculations.*

C_1	C_2	C_3	C_4	C_5	C_6	C_7^{eff}	C_9	C_{10}	$C^{(0)}$
-0.240	$+1.103$	$+0.011$	-0.025	$+0.007$	-0.030	-0.311	$+4.153$	-4.546	$+0.381$

Table 2: *Values of the Wilson coefficients used in the numerical calculations corresponding to the central values of the parameters given in Table 1. Here, $C_7^{\text{eff}} \equiv C_7 - C_5/3 - C_6$, and for C_9 we use the NDR scheme.*

3.1 Hadron energy spectrum

The explicit order α_s correction to O_9 can be obtained by using the existing results in the literature as follows: The vector current O_9 can be decomposed as $V = (V-A)/2 + (V+A)/2$. We recall that the $(V-A)$ and $(V+A)$ currents yield the same hadron energy spectrum [41] and there is no interference term present in this spectrum for massless leptons. So, the correction for the vector current case in $B \to X_s \ell^+ \ell^-$can be taken from the corresponding result for the charged $(V-A)$ case [28,40], yielding

$$C_9^{\text{eff}}(x_0) = C_9 \rho(x_0) + Y(x_0) \tag{26}$$

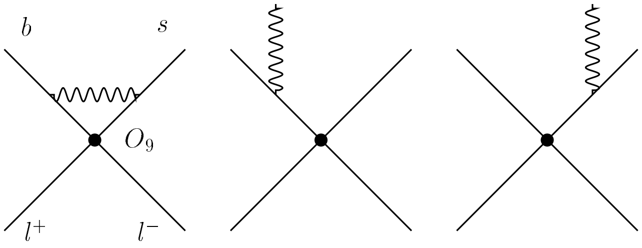

Figure 1: *Feynman diagrams contributing to the explicit order α_s corrections of the operator O_9. Curly lines denote a gluon. Wave function corrections are not shown.*

with

$$\rho(x) = 1 + \frac{\alpha_s}{\pi}\sigma(x), \tag{27}$$

$$\sigma(x) = \frac{1}{(3x - 4x^2 - 2\hat{m}_s^2 + 3\hat{m}_s^2 x)} \frac{G_1(x)}{3\sqrt{x^2 - \hat{m}_s^2}} , \tag{28}$$

where $Y(x_0) \equiv Y(\hat{s})$ with $\hat{s} = 1 - 2x_0 + \hat{m}_s^2$. The expression for $G_1(x)$ with $m_s \neq 0$ has been calculated in [40]. The effect of a finite m_s is negligible in $G_1(x)$, as can be seen in Fig. 2, where this function is plotted both with a finite s-quark mass, $m_s = 0.2$ GeV, and for the massless case, $m_s = 0$. A numerical difference occurs at the lowest order end point $x_0^{max} = 1/2(1 + \hat{m}_s^2)$ (for $m_l = 0$), where the function develops a singularity from above ($x_0 > x_0^{max}$) and the position of which depends on the value of m_s. The function $G_1(x)$ for a massless s-quark is given and discussed below [40].

$$\begin{aligned} G_1(x) &= x^2\{\frac{1}{90}(16x^4 - 84x^3 + 585x^2 - 1860x + 1215) + (8x-9)\ln(2x) \\ &+ 2(4x-3)\left[\frac{\pi^2}{2} + Li_2(1-2x)\right]\} \text{ for } 0 \leq x \leq 1/2 \ , \\ G_1(x) &= \frac{1}{180}(1-x)(32x^5 - 136x^4 + 1034x^3 - 2946x^2 + 1899x + 312) \\ &- \frac{1}{24}\ln(2x-1)(64x^3 - 48x^2 - 24x - 5) \\ &+ x^2(3-4x)\left[\frac{\pi^2}{3} - 4Li_2(\frac{1}{2x}) + \ln^2(2x-1) - 2\ln^2(2x)\right] \text{ for } 1/2 < x \leq 1 \ , \end{aligned} \tag{29}$$

where $Li_2(z)$ is the dilogarithmic function.

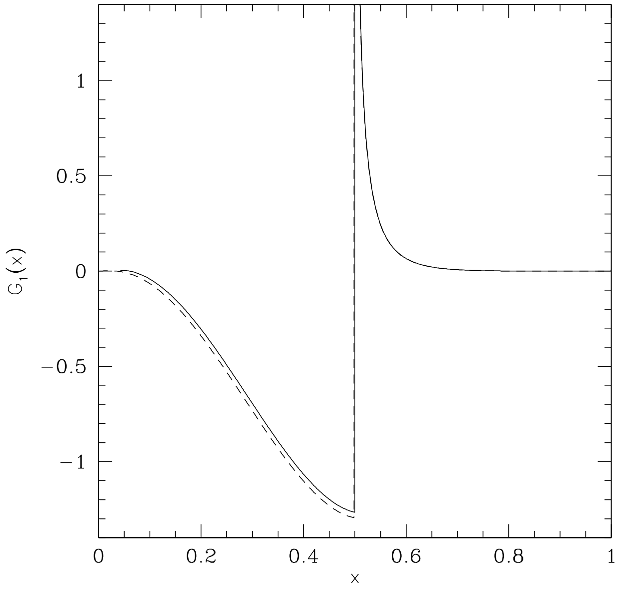

Figure 2: *The function* $G_1(x)$ *is shown for* $m_s = 0.2\,\mathrm{GeV}$ *(solid line) and for the massless case corresponding to eq. (29) (dashed line).*

The $\mathcal{O}(\alpha_s)$ correction has a double logarithmic (integrable) singularity for $x_0 \to 1/2$ from above ($x_0 > 1/2$). Further, the value of the order α_s corrected Wilson coefficient $C_9^{\text{eff}}(x_0)$ is reduced compared to its value with $\alpha_s = 0$, therefore also the hadron energy spectrum is reduced after including the explicit order α_s QCD correction for $0 < x_0 < 1/2$. Note that the hadron energy spectrum for $B \to X_s \ell^+ \ell^-$receives contributions for $1 \geq x > 1/2$ only from the order α_s bremsstrahlung corrections.

3.2 Hadronic invariant mass spectrum

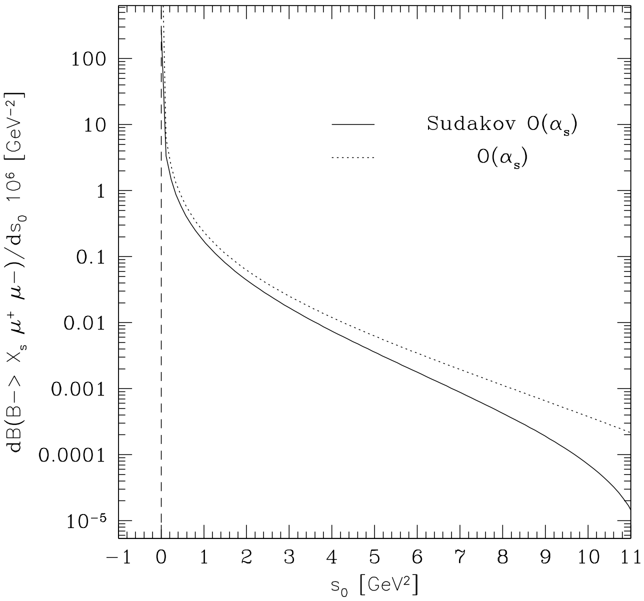

Figure 3: *The differential branching ratio* $\frac{\mathrm{d}\mathcal{B}(B\to X_s\ell^+\ell^-)}{\mathrm{d}s_0}$ *in the parton model is shown in the* $\mathcal{O}(\alpha_s)$ *bremsstrahlung region. The dotted (solid) line corresponds to eq. (30), (eq. (35)). The vertical line denotes the one particle pole from* $b \to s\ell^+\ell^-$. *We do not show the full spectra in the range* $0 \leq s_0 \leq m_b^2$ *as they tend to zero for larger values of* s_0.

We have calculated the order α_s perturbative QCD correction for the hadronic invariant mass in the range $\hat{m}_s^2 < \hat{s}_0 \leq 1$. Since the decay $b \to s + \ell^+ + \ell^-$ contributes in the parton model only at $\hat{s}_0 = \hat{m}_s^2$, only the bremsstrahlung graphs $b \to s + g + \ell^+ + \ell^-$ contribute in this range. This makes the calculation much simpler than in the full $\hat{s}_0$ range including virtual gluon diagrams. We find

$$\frac{\mathrm{d}\mathcal{B}}{\mathrm{d}\hat{s}_0} = \frac{2}{3}\mathcal{B}_0 \frac{\alpha_s}{\pi}\frac{1}{\hat{s}_0}\{\frac{(\hat{s}_0 - 1)}{27}(93 - 41\hat{s}_0 - 95\hat{s}_0^2 + 55\hat{s}_0^3) + \frac{4}{9}\ln\hat{s}_0(-3 - 5\hat{s}_0 + 9\hat{s}_0^2 - 2\hat{s}_0^4)\}C_9^2 \ . \tag{30}$$

Our result for the spectrum in $B \to X_s \ell^+ \ell^-$is in agreement with the corresponding result for the $(V - A)$ current obtained for the decay $B \to X_q \ell \nu_\ell$ in the $m_q = 0$ limit in ref. [32] (their eq. (3.8)), once one takes into account the difference in the normalizations. We display the hadronic invariant mass distribution in Fig. 3 as a function of s_0 (with $s_0 = m_b^2 \hat{s}_0$), where we also show the Sudakov improved spectrum, obtained from the $\mathcal{O}(\alpha_s)$ spectrum in which the double logarithms have been resummed. For the decay $B \to X_u \ell \nu_\ell$, this has been derived in ref. [33], where all further details

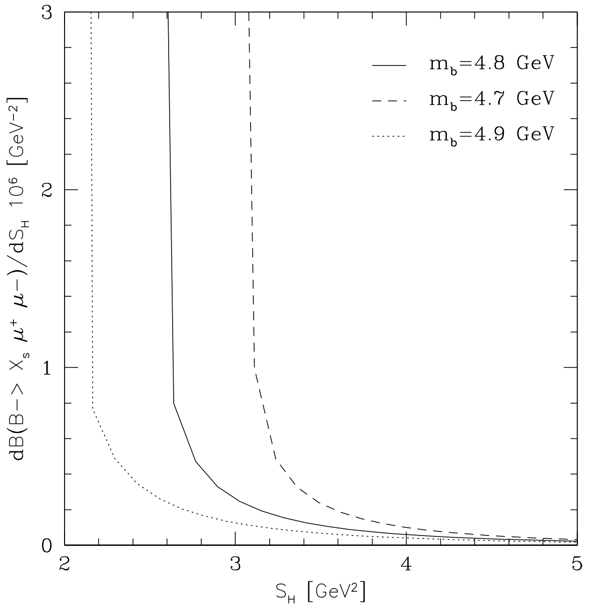

Figure 4: *The differential branching ratio* $\frac{\mathrm{d}\mathcal{B}(B\to X_s\ell^+\ell^-)}{\mathrm{d}S_H}$ *in the hadronic invariant mass,* S_H*, shown for different values of* m_b *in the range where only bremsstrahlung diagrams contribute. We do not show the result in the full kinematic range as the spectra tend monotonically to zero for larger values of* $S_H \le m_B^2$.

can be seen. We confirm eq. (17) of ref. [33] for the Sudakov exponentiated double differential decay rate $\frac{\mathrm{d}^2\Gamma}{\mathrm{d}x\mathrm{d}y}$ and use it after changing the normalization $\Gamma_0 \to \mathcal{B}_0\frac{2}{3}C_9^2$ for the decay $B \to X_s\ell^+\ell^-$. The constant $\mathcal{B}_0$ is given later. Defining the kinematic variables (x, y) as

$$\begin{aligned} q^2 &= x^2 m_b^2\,, \\ v\cdot q &= (x + \frac{1}{2}(1-x)^2 y)m_b\,, \end{aligned} \tag{31}$$

the Sudakov-improved Dalitz distribution is given by

$$\begin{aligned} \frac{d^2\mathcal{B}}{dxdy}(B\to X_s\ell^+\ell^-) &= -\mathcal{B}_0\frac{8}{3}x(1-x^2)^2(1+2x^2)\,\exp\Big(-\frac{2\alpha_s}{3\pi}\ln^2(1-y)\Big) \\ &\times \Big\{\frac{4\alpha_s}{3\pi}\frac{\ln(1-y)}{(1-y)}\Big[1-\frac{2\alpha_s}{3\pi}(G(x)+H(y))\Big]-\frac{2\alpha_s}{3\pi}\frac{dH}{dy}(y)\Big\}\,C_9^2\,, \end{aligned} \tag{32}$$

where [33]

$$\begin{aligned} G(x) &= \frac{[8x^2(1-x^2-2x^4)\ln x + 2(1-x^2)^2(5+4x^2)\ln(1-x^2) - (1-x^2)(5+9x^2-6x^4)]}{2(1-x^2)^2(1+2x^2)} \\ &\quad +\pi^2 + 2Li_2(x^2) - 2Li_2(1-x^2) \quad , \qquad (33) \\ H(y) &= \int_0^y dz\Big(\frac{4}{1-z}\ln\frac{2-z(1-x)+\kappa}{2} \\ &\quad -\frac{(1-x)(3+x+xz-z)}{(1+x)^2}\Big[\ln(1-z) - 2\ln\frac{2-z(1-x)+\kappa}{2}\Big] \end{aligned}$$

$$-\frac{\kappa}{2(1+x)^2(1+2x^2)}\Big[\frac{7(1+x)(1+2x^2)}{1-z}+(1-x)(3-2x^2)\Big]\Big) \,. \qquad (34)$$

The quantity κ in eq. (34) is defined as $\kappa \equiv \sqrt{z^2(1-x)^2+4xz}$.

To get the hadronic invariant mass spectrum for a b quark decaying at rest we change variables from (x,y) to (q^2,s_0) followed by an integration over q^2,

$$\frac{\mathrm{d}\mathcal{B}}{\mathrm{d}s_0} = \int_{4m_l^2}^{(m_b-\sqrt{s_0})^2} \mathrm{d}q^2 \frac{\mathrm{d}^2\mathcal{B}}{\mathrm{d}x\mathrm{d}y}\frac{1}{2m_b^4 x(1-x)^2} \,. \qquad (35)$$

The most significant effect of the bound state is the difference between m_B and m_b, which is dominated by $\bar{\Lambda}$. Neglecting λ_1, λ_2, i.e., using $\bar{\Lambda} = m_B - m_b$, the spectrum $\frac{\mathrm{d}\mathcal{B}}{\mathrm{d}S_H}$ is obtained along the lines as given above for $\frac{d\mathcal{B}}{ds_0}$, after changing variables from (x,y) to (q^2,S_H) and performing an integration over q^2. It is valid in the region $m_B\frac{m_B\bar{\Lambda}-\bar{\Lambda}^2+m_s^2}{m_B-\bar{\Lambda}} < S_H \leq m_B^2$ (or $m_B\bar{\Lambda} \leq S_H \leq m_B^2$, neglecting m_s) which excludes the zeroth order and virtual gluon kinematics ($s_0 = m_s^2$), yielding

$$\frac{\mathrm{d}\mathcal{B}}{\mathrm{d}S_H} = \int_{4m_l^2}^{(m_B-\sqrt{S_H})^2} \mathrm{d}q^2 \frac{\mathrm{d}^2\mathcal{B}}{\mathrm{d}x\mathrm{d}y}\frac{1}{2m_b^3 m_B x(1-x)^2} \,. \qquad (36)$$

The hadronic invariant mass spectrum thus found depends rather sensitively on m_b (or equivalently $\bar{\Lambda}$), as can be seen from Fig. 4. An analogous analysis for the charged current semileptonic B decays $B \to X_u \ell \nu_\ell$ has been performed in ref. [34], with similar conclusions.

4 Power Corrections in the Decay $B \to X_s \ell^+ \ell^-$

The hadronic tensor in eq. (25) can be expanded in inverse powers of m_b with the help of the HQET techniques. The leading term in this expansion, i.e., $\mathcal{O}(m_b^0)$ reproduces the parton model result. In HQET, the next to leading power corrections are parameterized in terms of the matrix elements of the kinetic energy and the magnetic moment operators λ_1 and λ_2, respectively. The $B-B^*$ mass difference yields the value $\lambda_2 = 0.12$ GeV^2. In all numerical estimates we shall use this value of λ_2 and, unless otherwise stated, we take the value for λ_1 extracted from an analysis of data on semileptonic B-decays ($B \to X \ell \nu_\ell$), yielding $\lambda_1 = -0.20$ GeV^2 with a corresponding value $\bar{\Lambda} = 0.39$ GeV [37]. For a review on the dispersion in the present values of these non-perturbative parameters, see [38].

The contributions of the power corrections to the structure functions T_i can be decomposed into the sum of various terms, denoted by $T_i^{(j)}$, which can be traced back to well defined pieces in the evaluation of the time-ordered product in eq. (23):

$$T_i(v.\hat{q},\hat{s}) = \sum_{j=0,1,2,s,g,\delta} T_i^{(j)}(v.\hat{q},\hat{s}) \,. \qquad (37)$$

The expressions for $T_i^{(j)}(v.\hat{q},\hat{s})$, $i = 1,2,3$ calculated up to $O(m_B/m_b^3)$ are given in [15]. After contracting the hadronic and leptonic tensors, one finds

$$T^{L/R}{}_{\mu\nu}\, L^{L/R^{\mu\nu}} = {m_b}^2 \left\{ 2\,\hat{s}\,{T_1}^{L/R} + \left[(v\cdot\hat{q})^2 - \frac{1}{4}\hat{u}^2 - \hat{s}\right] {T_2}^{L/R} \mp \hat{s}\,\hat{u}\,{T_3}^{L/R} \right\} \,. \qquad (38)$$

With the help of the kinematic identities given in eq. (7), we can make the dependence on x_0 and $\hat{s}_0$ explicit,

$$T^{L/R}{}_{\mu\nu}\, L^{L/R\mu\nu} = {m_b}^2 \left\{ 2(1-2x_0+\hat{s}_0){T_1}^{L/R} + \left[x_0^2 - \frac{1}{4}\hat{u}^2 - \hat{s}_0\right] {T_2}^{L/R} \mp (1-2x_0+\hat{s}_0)\hat{u}\, {T_3}^{L/R} \right\} \tag{39}$$

and with this we are able to derive the double differential power corrected spectrum $\frac{\mathrm{d}\mathcal{B}}{\mathrm{d}x_0\,\mathrm{d}\hat{s}_0}$ for $B \to X_s \ell^+ \ell^-$. Integrating eq. (22) over $\hat{u}$ first, where the variable $\hat{u}$ is bounded by

$$-2\sqrt{x_0^2-\hat{s}_0} \le \hat{u} \le +2\sqrt{x_0^2-\hat{s}_0}\ , \tag{40}$$

we arrive at the following expression

$$\frac{\mathrm{d}^2\mathcal{B}}{\mathrm{d}x_0\,\mathrm{d}\hat{s}_0} \;=\; -\frac{8}{\pi}\mathcal{B}_0 \mathrm{Im}\sqrt{x_0^2-\hat{s}_0}\left\{(1-2x_0+\hat{s}_0)T_1(\hat{s}_0,x_0) + \frac{x_0^2-\hat{s}_0}{3}T_2(\hat{s}_0,x_0)\right\} + \mathcal{O}(\lambda_i\alpha_s)\,, \tag{41}$$

where

$$\begin{aligned}
T_1(\hat{s}_0,x_0) \;=\;& \frac{1}{x}\Bigg\{ \left(8x_0 - 4(\frac{\hat{\lambda}_1}{3}+\hat{\lambda}_2)\right)\left(|C_9^{\mathrm{eff}}(\hat{s})|^2 + |C_{10}|^2\right) \\
+\;& \Bigg(32(-2\hat{m}_s^2 - 2\hat{s}_0 - 4\hat{m}_s^2\hat{s}_0 + x_0 + 5\hat{m}_s^2x_0 + \hat{s}_0x_0 + \hat{m}_s^2\hat{s}_0x_0) + 16(\frac{\hat{\lambda}_1}{3}+\hat{\lambda}_2) \\
\times\;& (-5 - 11\hat{m}_s^2 + 5\hat{s}_0 - \hat{m}_s^2\hat{s}_0 + 10x_0 + 22\hat{m}_s^2x_0 - 10x_0^2 - 10\hat{m}_s^2x_0^2)\Bigg)\frac{|C_7^{\mathrm{eff}}|^2}{(\hat{s}_0-2x_0+1)^2} \\
+\;& \left(\frac{-32}{\hat{s}_0-2x_0+1}(\hat{m}_s^2 + \hat{s}_0 - x_0 - \hat{m}_s^2x_0) - 48(\frac{\hat{\lambda}_1}{3}+\hat{\lambda}_2)\right) Re(C_9^{\mathrm{eff}}(\hat{s}))\, C_7^{\mathrm{eff}} \Bigg\} \\
+\;& \frac{1}{x^2}\Bigg\{ \left(\frac{8\hat{\lambda}_1}{3}(-2\hat{s}_0 - 3x_0 + 5x_0^2) + 8\hat{\lambda}_2(-2\hat{s}_0 + x_0 + 5x_0^2)\right)\left(|C_9^{\mathrm{eff}}(\hat{s})|^2 + |C_{10}|^2\right) \\
+\;& \Bigg(\frac{32\hat{\lambda}_1}{3}(6\hat{m}_s^2 + 12\hat{s}_0 + 18\hat{m}_s^2\hat{s}_0 - 2\hat{s}_0^2 - 2\hat{m}_s^2\hat{s}_0^2 - 3x_0 - 21\hat{m}_s^2x_0 - 13\hat{s}_0x_0 - 19\hat{m}_s^2\hat{s}_0x_0 \\
-\;& 3x_0^2 + 9\hat{m}_s^2x_0^2 + 5\hat{s}_0x_0^2 + 5\hat{m}_s^2\hat{s}_0x_0^2 + 4x_0^3 + 4\hat{m}_s^2x_0^3) \\
+\;& 32\hat{\lambda}_2(-2\hat{m}_s^2 - 2\hat{m}_s^2\hat{s}_0 - 2\hat{s}_0^2 - 2\hat{m}_s^2\hat{s}_0^2 + x_0 - \hat{m}_s^2x_0 - 5\hat{s}_0x_0 - 11\hat{m}_s^2\hat{s}_0x_0 + x_0^2 \\
+\;& 13\hat{m}_s^2x_0^2 + 5\hat{s}_0x_0^2 + 5\hat{m}_s^2\hat{s}_0x_0^2)\Bigg)\frac{|C_7^{\mathrm{eff}}|^2}{(\hat{s}_0-2x_0+1)^2} \\
+\;& \Bigg(\frac{-32\hat{\lambda}_1}{3}(-3\hat{m}_s^2 - 5\hat{s}_0 + 2\hat{m}_s^2\hat{s}_0 + 3x_0 + 6\hat{m}_s^2x_0 + 3\hat{s}_0x_0 - x_0^2 - 5\hat{m}_s^2x_0^2) \\
-\;& 32\hat{\lambda}_2(\hat{m}_s^2 + \hat{s}_0 + 2\hat{m}_s^2\hat{s}_0 - x_0 + 2\hat{m}_s^2x_0 + 3\hat{s}_0x_0 - 3x_0^2 - 5\hat{m}_s^2x_0^2)\Bigg)\frac{Re(C_9^{\mathrm{eff}}(\hat{s}))\, C_7^{\mathrm{eff}}}{\hat{s}_0-2x_0+1}\Bigg\} \\
+\;& \frac{1}{x^3}\hat{\lambda}_1(\hat{s}_0 - x_0^2)\Bigg\{\frac{32x_0}{3}\left(|C_9^{\mathrm{eff}}(\hat{s})|^2 + |C_{10}|^2\right) \\
+\;& \frac{128}{3}(-2\hat{m}_s^2 - 2\hat{s}_0 - 4\hat{m}_s^2\hat{s}_0 + x_0 + 5\hat{m}_s^2x_0 + \hat{s}_0x_0 + \hat{m}_s^2\hat{s}_0x_0)\frac{|C_7^{\mathrm{eff}}|^2}{(\hat{s}_0-2x_0+1)^2} \\
+\;& \frac{-128}{3}(\hat{m}_s^2 + \hat{s}_0 - x_0 - \hat{m}_s^2x_0)\frac{Re(C_9^{\mathrm{eff}}(\hat{s}))\, C_7^{\mathrm{eff}}}{\hat{s}_0-2x_0+1}\Bigg\}\ ,
\end{aligned}$$

$$\begin{aligned} T_2(\hat{s}_0, x_0) &= \frac{1}{x}\left\{\left(16 - 40(\frac{\hat{\lambda}_1}{3} + \hat{\lambda}_2)\right)\left(|C_9^{\rm eff}(\hat{s})|^2 + |C_{10}|^2\right) + \left(-64 + 160(\frac{\hat{\lambda}_1}{3} + \hat{\lambda}_2)\right)(1 + \hat{m}_s^2)\frac{|C_7^{\rm eff}|^2}{\hat{s}_0 - 2x_0 + 1}\right\} \\ &+ \frac{1}{x^2}\left\{\left(\frac{112\hat{\lambda}_1}{3}(-1 + x_0) + 16\hat{\lambda}_2(-3 + 5x_0)\right)\left(|C_9^{\rm eff}(\hat{s})|^2 + |C_{10}|^2\right)\right. \\ &+ \left.\left(\frac{448\hat{\lambda}_1}{3}(1 - x_0) + 64\hat{\lambda}_2(5x_0 - 1)\right)(1 + \hat{m}_s^2)\frac{|C_7^{\rm eff}|^2}{\hat{s}_0 - 2x_0 + 1} - 64\hat{\lambda}_2 Re(C_9^{\rm eff}(\hat{s}))\, C_7^{\rm eff}\right\} \\ &+ \frac{1}{x^3}\hat{\lambda}_1(\hat{s}_0 - x_0^2)\left\{\frac{64}{3}\left(|C_9^{\rm eff}(\hat{s})|^2 + |C_{10}|^2\right) + \frac{-256}{3}(1 + \hat{m}_s^2)\frac{|C_7^{\rm eff}|^2}{\hat{s}_0 - 2x_0 + 1}\right\} . \end{aligned} \tag{42}$$

Here, $x = \hat{s}_0 - \hat{m}_s^2 + i\epsilon$, $\hat{\lambda}_1 = \lambda_1/m_b^2$ and $\hat{\lambda}_2 = \lambda_2/m_b^2$. As the structure function T_3 does not contribute to the branching ratio, we did not consider it in our present work. The Wilson coefficient $C_9^{\rm eff}(\hat{s})$ depends both on the variables x_0 and $\hat{s}_0$ arising from the matrix element of the Four-Fermi-operators.

The branching ratio for $B \to X_s \ell^+ \ell^-$is usually expressed in terms of the measured semileptonic branching ratio $\mathcal{B}_{sl}$ for the decays $B \to X_c \ell \nu_\ell$. This fixes the normalization constant $\mathcal{B}_0$ to be,

$$\mathcal{B}_0 \equiv \mathcal{B}_{sl}\frac{3\,\alpha^2}{16\pi^2}\frac{|V_{ts}^* V_{tb}|^2}{|V_{cb}|^2}\frac{1}{f(\hat{m}_c)\kappa(\hat{m}_c)} , \tag{43}$$

where

$$f(\hat{m}_c) = 1 - 8\,\hat{m}_c^2 + 8\,\hat{m}_c^6 - \hat{m}_c^8 - 24\,\hat{m}_c^4\,\ln\hat{m}_c \tag{44}$$

is the phase space factor for $\Gamma(B \to X_c \ell \nu_\ell)$ and the function $\kappa(\hat{m}_c)$ accounts for both the $O(\alpha_s)$ QCD correction to the semileptonic decay width [42] and the leading order $(1/m_b)^2$ power correction [16]. It reads as:

$$\kappa(\hat{m}_c) = 1 + \frac{\alpha_s(m_b)}{\pi}g(\hat{m}_c) + \frac{h(\hat{m}_c)}{2m_b^2} , \tag{45}$$

where

$$g(\hat{m}_c) = \frac{A_0(\hat{m}_c)}{f(\hat{m}_c)} , \tag{46}$$

$$h(\hat{m}_c) = \lambda_1 + \frac{\lambda_2}{f(\hat{m}_c)}\left[-9 + 24\hat{m}_c^2 - 72\hat{m}_c^4 + 72\hat{m}_c^6 - 15\hat{m}_c^8 - 72\hat{m}_c^4\ln\hat{m}_c\right] , \tag{47}$$

and the analytic form of $A_0(\hat{m}_c)$ can be seen in [32]. Note that the frequently used approximation $g(z) \approx -\frac{2}{3}((\pi^2 - \frac{31}{4})(1-z)^2 + \frac{3}{2})$ holds within 1.4% accuracy in the range $0.2 \leq z \leq 0.4$. The equation $g(z) = -1.671 + 2.04(z - 0.3) - 2.15(z - 0.3)^2$ is accurate for $0.2 \leq z \leq 0.4$ to better than one per mille accuracy and that is what we have used here.

The double differential ratio given in eq. (41) agrees in the $(V - A)$ limit with the corresponding expression derived for the semileptonic decay $B \to X_c \ell \nu_\ell$ in [32] (their eq. (3.2)). Taking this limit amounts to the following transcription:

$$C_9^{\rm eff} = -C_{10} = \frac{1}{2} , \tag{48}$$

$$C_7^{\rm eff} = 0 , \tag{49}$$

$$\left(\frac{G_F\,\alpha}{\sqrt{2}\,\pi}V_{ts}^* V_{tb}\right) \to \left(-\frac{4\,G_F}{\sqrt{2}}V_{cb}\right) . \tag{50}$$

The hadron energy spectrum can now be obtained by integrating over $\hat{s}_0$. The imaginary part can be obtained using the relation:

$$\mathrm{Im}\frac{1}{x^n} \propto \frac{(-1)^{n-1}}{(n-1)!}\delta^{(n-1)}(\hat{s}_0 - \hat{m}_s^2) \ . \tag{51}$$

The kinematic boundaries are given as:

$$\begin{aligned} max(\hat{m}_s^2, -1 + 2x_0 + 4\hat{m}_l^2) \leq \ \ & \hat{s}_0 \ \ \leq x_0^2 \ , \\ \hat{m}_s \leq \ \ & x_0 \ \ \leq \frac{1}{2}(1 + \hat{m}_s^2 - 4\hat{m}_l^2) \ . \end{aligned} \tag{52}$$

Here we keep $\hat{m}_l$ as a regulator wherever it is necessary and abbreviate $C_9^{\rm eff} \equiv C_9^{\rm eff}(\hat{s} = 1 - 2x_0 + \hat{m}_s^2)$. Including the leading power corrections, the hadron energy spectrum in the decay $B \to X_s \ell^+ \ell^-$is given below:

$$\begin{aligned} \frac{\mathrm{d}\mathcal{B}}{\mathrm{d}x_0} \ = \ & \mathcal{B}_0 \Big\{ \left[g_0^{(9,10)} + \hat{\lambda}_1 g_1^{(9,10)} + \hat{\lambda}_2 g_2^{(9,10)}\right] \left(|C_9^{\rm eff}|^2 + |C_{10}|^2\right) \\ + \ & \left[g_0^{(7)} + \hat{\lambda}_1 g_1^{(7)} + \hat{\lambda}_2 g_2^{(7)}\right] \frac{|C_7^{\rm eff}|^2}{x_0 - \frac{1}{2}(1 + \hat{m}_s^2)} + \left[g_0^{(7,9)} + \hat{\lambda}_1 g_1^{(7,9)} + \hat{\lambda}_2 g_2^{(7,9)}\right] Re(C_9^{\rm eff})\, C_7^{\rm eff} \\ + \ & (\hat{\lambda}_1 h_1^{(9)} + \hat{\lambda}_2 h_2^{(9)}) \frac{d|C_9^{\rm eff}|^2}{d\hat{s}_0} + \hat{\lambda}_1 k_1^{(9)} \frac{d^2|C_9^{\rm eff}|^2}{d\hat{s}_0^2} \\ + \ & (\hat{\lambda}_1 h_1^{(7,9)} + \hat{\lambda}_2 h_2^{(7,9)}) \frac{dRe(C_9^{\rm eff})}{d\hat{s}_0}\, C_7^{\rm eff} + \hat{\lambda}_1 k_1^{(7,9)} \frac{d^2 Re(C_9^{\rm eff})}{d\hat{s}_0^2}\, C_7^{\rm eff} \Big\} \\ + \ & \delta(x_0 - \frac{1}{2}(1 + \hat{m}_s^2 - 4\hat{m}_l^2)) f_\delta(\hat{\lambda}_1, \hat{\lambda}_2) + \delta'(x_0 - \frac{1}{2}(1 + \hat{m}_s^2 - 4\hat{m}_l^2)) f_{\delta'}(\hat{\lambda}_1, \hat{\lambda}_2) \ . \end{aligned} \tag{53}$$

The functions $g_i^{(9,10)}, g_i^{(7)}, g_i^{(7,9)}, h_i^{(9)}, h_i^{(7,9)}, k_1^{(9)}, k_1^{(7,9)}$ in the above expression are the coefficients of the $1/m_b^2$ power expansion for different combinations of Wilson coefficients, with $g_0^{(j,k)}$ being the lowest order (parton model) functions. They are functions of the variables x_0 and $\hat{m}_s$ and are given in appendix A. The singular functions δ, δ' have support only at the lowest order end point of the spectrum, i.e., at $x_0^{max} \equiv \frac{1}{2}(1 + \hat{m}_s^2 - 4\hat{m}_l^2)$. The auxiliary functions $f_\delta(\hat{\lambda}_1, \hat{\lambda}_2)$ and $f_{\delta'}(\hat{\lambda}_1, \hat{\lambda}_2)$ vanish in the limit $\hat{\lambda}_1 = \hat{\lambda}_2 = 0$. They are given in appendix B. The derivatives of $C_9^{\rm eff}$ are defined as $\frac{d^n C_9^{\rm eff}}{d\hat{s}_0^n} \equiv \frac{d^n C_9^{\rm eff}}{d\hat{s}^n}(\hat{s} = 1 - 2x_0 + \hat{s}_0; \hat{s}_0 = \hat{m}_s^2)$ $(n = 1, 2)$. In the $(V - A)$ limit our eq. (53) for the hadron energy spectrum in $B \to X_s \ell^+ \ell^-$agrees with the corresponding spectrum in $B \to X \ell \nu_\ell$ given in [32] (their eq. (A1)). Integrating also over x_0 the resulting total width for $B \to X_s \ell^+ \ell^-$agrees again in the $(V - A)$ limit with the well known result [16].

The power-corrected hadron energy spectrum $\frac{\mathrm{d}\mathcal{B}(B \to X_s \ell^+ \ell^-)}{\mathrm{d}E_0}$ (with $E_0 = m_b x_0$) is displayed in Fig. 5 through the solid curve, however, without the singular δ, δ' terms. Note that before reaching the kinematic lower end point, the power-corrected spectrum becomes negative, as a result of the $\hat{\lambda}_2$ term. This behavior is analogous to what has already been reported for the dilepton mass spectrum $\frac{\mathrm{d}\mathcal{B}(B \to X_s \ell^+ \ell^-)}{\mathrm{d}q^2}$ in the high q^2 region [15], signaling a breakdown of the $\frac{1}{m_b}$ expansion in this region. The

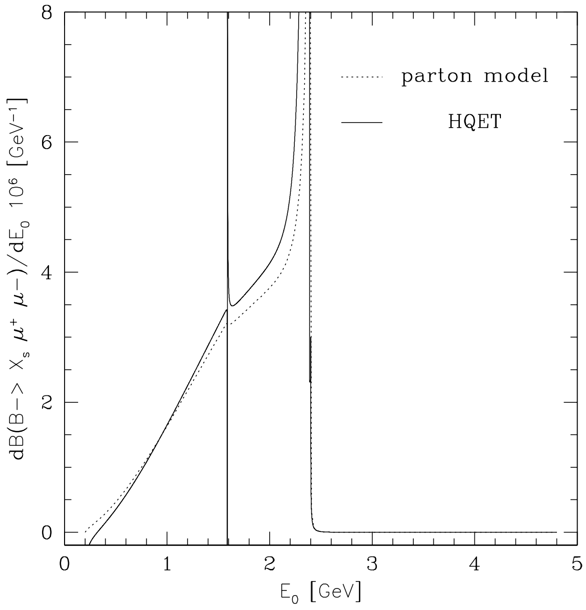

Figure 5: *Hadron energy spectrum* $\frac{\mathrm{d}\mathcal{B}(B \to X_s \ell^+ \ell^-)}{\mathrm{d}E_0}$ *in the parton model (dotted line) and including leading power corrections (solid line). For* $m_b/2 < E_0 \leq m_b$ *the distributions coincide. The parameters used for this plot are the central values given in Table 1 and the default values of the HQET parameters specified in text.*

terms with the derivatives of C_9^{eff} in eq. (53) give rise to a singularity in the hadron energy spectrum at the charm threshold due to the cusp in the function $Y(\hat{s})$, when approached from either side. The hadron energy spectrum for the parton model is also shown in Fig. 5, which is finite for all ranges of E_0.

What is the region of validity of the hadron energy spectrum derived in HQET? It is known that in $B \to X_s \ell^+ \ell^-$decay there are resonances present, from which the known six [6] populate the x_0 (or E_0) range between the lower end point and the charm threshold. Taking this into account and what has been remarked earlier, one concludes that the HQET spectrum cannot be used near the resonances, near the charm threshold and around the lower endpoint. Excluding these regions, the spectrum calculated in HQET is close to the (partonic) perturbative spectrum as the power corrections are shown to be small. The authors of ref. [20], [1] who have performed an $1/m_c$ expansion for the dilepton mass spectrum $\frac{\mathrm{d}\mathcal{B}(B \to X_s \ell^+ \ell^-)}{\mathrm{d}q^2}$ and who also found a charm-threshold singularity, expect a reliable prediction of the spectrum for $q^2 \leq 3m_c^2$ corresponding to $E_0 \geq \frac{m_b}{2}(1 + \hat{m}_s^2 - 3\hat{m}_c^2) \approx 1.8$ GeV. In this region, the effect of the $1/m_b$ power corrections on the energy spectrum is small and various spectra in $B \to X_s \ell^+ \ell^-$calculated here and in ref. [15] can be compared with data.

---

[1] The $\mathcal{O}(1/m_c^2)$ correction to $\frac{\mathrm{d}\mathcal{B}(B \to X_s \ell^+ \ell^-)}{\mathrm{d}q^2}$ has also been calculated in ref. [21], however, the result differs in sign from the one in ref. [20]. It seems that this controversy has been settled in favor of ref. [20].

The leading power corrections to the invariant mass spectrum is found by integrating eq. (41) with respect to x_0. We have already discussed the non-trivial hadronic invariant mass spectrum which results from the $\mathcal{O}(\alpha_s)$ bremsstrahlung and its Sudakov-improved version. Since we have consistently dropped everywhere terms of $\mathcal{O}(\lambda_i\alpha_s)$ (see eq. (41)), this is the only contribution to the invariant mass spectrum also in HQET away from $\hat{s}_0 = \hat{m}_s^2$, as the result of integrating the terms involving power corrections in eq. (41) over x_0 is a singular function with support only at $\hat{s}_0 = \hat{m}_s^2$. Of course, these corrections contribute to the normalization (i.e., branching ratio) but leave the perturbative spectrum intact for $\hat{s}_0 \neq \hat{m}_s^2$.

5 Hadronic Moments in $B \to X_s\ell^+\ell^-$ in HQET

We start with the derivation of the lowest spectral moments in the decay $B \to X_s\ell^+\ell^-$at the parton level. These moments are worked out by taking into account the two types of corrections discussed earlier, namely the leading power $1/m_b$ and the perturbative $\mathcal{O}(\alpha_s)$ corrections. To that end, we define:

$$\mathcal{M}_{l^+l^-}^{(n,m)} \equiv \frac{1}{\mathcal{B}_0}\int (\hat{s}_0-\hat{m}_s^2)^n x_0^m \, \frac{\mathrm{d}^2\mathcal{B}}{\mathrm{d}\hat{s}_0\mathrm{d}x_0}\, \mathrm{d}\hat{s}_0\mathrm{d}x_0\,, \tag{54}$$

for integers n and m. These moments are related to the corresponding moments $\langle x_0^m(\hat{s}_0-\hat{m}_s^2)^n\rangle$ obtained at the parton level by a scaling factor which yields the corrected branching ratio $\mathcal{B} = \mathcal{B}_0\mathcal{M}_{\ell^+\ell^-}^{(n,m)}$. Thus,

$$\langle x_0^m(\hat{s}_0-\hat{m}_s^2)^n\rangle = \frac{\mathcal{B}_0}{\mathcal{B}}\,\mathcal{M}_{l^+l^-}^{(n,m)}\,. \tag{55}$$

The correction factor $\mathcal{B}_0/\mathcal{B}$ is given a little later. We remind that one has to Taylor expand it in terms of the $\mathcal{O}(\alpha_s)$ and power corrections. The moments can be expressed as double expansion in $\mathcal{O}(\alpha_s)$ and $1/m_b$ and to the accuracy of our calculations can be represented in the following form:

$$\mathcal{M}_{l^+l^-}^{(n,m)} = D_0^{(n,m)} + \frac{\alpha_s}{\pi}{C_9}^2 A^{(n,m)} + \hat{\lambda}_1 D_1^{(n,m)} + \hat{\lambda}_2 D_2^{(n,m)}\ , \tag{56}$$

with a further decomposition into pieces from different Wilson coefficients for $i = 0, 1, 2$:

$$D_i^{(n,m)} = \alpha_i^{(n,m)} {C_7^{\mathrm{eff}}}^2 + \beta_i^{(n,m)} C_{10}^2 + \gamma_i^{(n,m)} C_7^{\mathrm{eff}} + \delta_i^{(n,m)}. \tag{57}$$

The terms $\gamma_i^{(n,m)}$ and $\delta_i^{(n,m)}$ in eq. (57) result from the terms proportional to $Re(C_9^{\mathrm{eff}})C_7^{\mathrm{eff}}$ and $|C_9^{\mathrm{eff}}|^2$ in eq. (41), respectively. The results for $\alpha_i^{(n,m)}, \beta_i^{(n,m)}, \gamma_i^{(n,m)}, \delta_i^{(n,m)}$ are presented in appendix C. Out of these, the functions $\alpha_i^{(n,m)}$ and $\beta_i^{(n,m)}$ are given analytically, but the other two $\gamma_i^{(n,m)}$ and $\delta_i^{(n,m)}$ are given in terms of a one-dimensional integral over x_0, as these latter functions involve the coefficient C_9^{eff}, which is a complicated function of x_0.

The leading perturbative contributions for the hadronic invariant mass and hadron energy moments can be obtained analytically by integrating eq. (30) and eq. (29), respectively, yielding

$$\begin{aligned} A^{(0,0)} &= \frac{25-4\pi^2}{9}\,, \quad A^{(1,0)} = \frac{91}{675}\,, \quad A^{(2,0)} = \frac{5}{486}\,, \\ A^{(0,1)} &= \frac{1381-210\pi^2}{1350}\,, A^{(0,2)} = \frac{2257-320\pi^2}{5400}\,. \end{aligned} \tag{58}$$

The zeroth moment $n = m = 0$ is needed for the normalization and we recall that the result for $A^{(0,0)}$ was derived by Cabibbo and Maiani in the context of the $\mathcal{O}(\alpha_s)$ correction to the semileptonic decay rate $B \to X\ell\nu_\ell$ quite some time ago [42]. Likewise, the first mixed moment $A^{(1,1)}$ can be extracted from the results given in [32] for the decay $B \to X\ell\nu_\ell$ after changing the normalization,

$$A^{(1,1)} = \frac{3}{50}\,. \tag{59}$$

For the lowest order parton model contribution $D_0^{(n,m)}$, we find, in agreement with [32], that the first two hadronic invariant mass moments $\langle \hat{s}_0 - \hat{m}_s^2 \rangle$, $\langle (\hat{s}_0 - \hat{m}_s^2)^2 \rangle$ and the first mixed moment $\langle x_0(\hat{s}_0 - \hat{m}_s^2) \rangle$ vanish:

$$D_0^{(n,0)} = 0 \;\text{ for } n = 1, 2 \;\text{ and }\; D_0^{(1,1)} = 0\,. \tag{60}$$

We remark that we have included the s-quark mass dependence in the leading term and in the power corrections, but omitted it throughout our work in the calculation of the explicit α_s term. All the expressions derived here for the moments agree in the $V-A$ limit (and with $\hat{m}_s = 0$ in the perturbative α_s correction term) with the corresponding expressions given in [32]. From here the full $\mathcal{O}(\alpha_s m_s)$ expressions can be inferred after adjusting the normalization $\Gamma_0 \to \mathcal{B}_0 \frac{2}{3} C_9^2$. We have checked that a finite s-quark mass effects the values of the $A^{(n,m)}$ given in eq. (58-59) by less than 8% for $m_s = 0.2$ GeV.

We can eliminate the hidden dependence on the non-perturbative parameters resulting from the b-quark mass in the moments $\mathcal{M}_{l^+l^-}^{(n,m)}$ with the help of the HQET mass relation. As m_s is of order Λ_{QCD}, to be consistent we keep only terms up to order m_s^2/m_b^2 [43]. An additional m_b-dependence is in the mass ratios $\hat{m}_l = \frac{m_l}{m_b}$. Substituting m_b by the B meson mass using the HQET relation introduces additional $\mathcal{O}(1/m_B, 1/m_B^2)$ terms in the Taylor expansion of eq. (55). We get for the following normalization factor for $\mathcal{B}/\mathcal{B}_0 = \mathcal{M}_{\ell^+\ell^-}^{(0,0)}$:

$$\begin{aligned} \frac{\mathcal{B}}{\mathcal{B}_0} &= \frac{32}{9m_B^2}(-4m_B^2 - 13m_s^2 - 3(m_B^2 - 2m_s^2)\ln(4\frac{m_l^2}{m_B^2}))C_7^{\mathrm{eff}^2} + \frac{2}{3m_B^2}(m_B^2 - 8m_s^2)C_{10}^2 \\ &+ \int_{m_s/m_B}^{\frac{1}{2}(1+m_s^2/m_B^2)} dx_0 \frac{64}{m_B^2}(-m_s^2 - 4m_s^2 x_0 + 2m_B^2 x_0^2 + 2m_s^2 x_0^2) Re(C_9^{\mathrm{eff}})C_7^{\mathrm{eff}} \\ &+ \int_{m_s/m_B}^{\frac{1}{2}(1+m_s^2/m_B^2)} dx_0 \frac{16}{3m_B^2}(-3m_s^2 + 6m_B^2 x_0^2 + 6m_s^2 x_0^2 - 8m_B^2 x_0^3)|C_9^{\mathrm{eff}}|^2 \end{aligned}$$

$$\begin{aligned} &+ \quad \frac{\alpha_s}{\pi} A^{(0,0)} C_9^2 + \frac{-64}{3} C_7^{\mathrm{eff}^2} \frac{\bar{\Lambda}}{m_B} + \frac{-32}{3} C_7^{\mathrm{eff}^2} \frac{\bar{\Lambda}^2}{m_B^2} + \left[\frac{16}{9} (2 - 3 \ln(4 \frac{m_l^2}{m_B^2})) C_7^{\mathrm{eff}^2} + \frac{C_{10}^2}{3} \right. \\ &+ \quad \left. \int_0^{\frac{1}{2}} dx_0 (64 x_0^2 Re(C_9^{\mathrm{eff}}) C_7^{\mathrm{eff}} + \frac{16}{3} (3 - 4x_0) x_0^2 |C_9^{\mathrm{eff}}|^2) \right] \frac{\lambda_1}{m_B^2} \\ &+ \quad \left[\frac{16}{3} (4 + 9 \ln(4 \frac{m_l^2}{m_B^2})) C_7^{\mathrm{eff}^2} - 3 C_{10}^2 \right. \qquad (61) \\ &+ \quad \left. \int_0^{\frac{1}{2}} dx_0 (64(-1 - 4x_0 + 7x_0^2) Re(C_9^{\mathrm{eff}}) C_7^{\mathrm{eff}} + 16(-1 + 15 x_0^2 - 20 x_0^3) |C_9^{\mathrm{eff}}|^2 \right] \frac{\lambda_2}{m_B^2} \, . \end{aligned}$$

Here, the $\frac{\bar{\Lambda}}{m_B}$ and $\frac{\bar{\Lambda}^2}{m_B^2}$ terms result from the expansion of $\ln(4m_l^2/m_b^2)$. The first two moments and the first mixed moment, $\langle x_0 \rangle \mathcal{B}/\mathcal{B}_0$, $\langle x_0^2 \rangle \mathcal{B}/\mathcal{B}_0$, $\langle \hat{s}_0 - \hat{m}_s^2 \rangle \mathcal{B}/\mathcal{B}_0$, $\langle (\hat{s}_0 - \hat{m}_s^2)^2 \rangle \mathcal{B}/\mathcal{B}_0$ and $\langle x_0 (\hat{s}_0 - \hat{m}_s^2) \rangle \mathcal{B}/\mathcal{B}_0$ are presented in appendix D.

With this we obtain the moments for the physical quantities valid up to $\mathcal{O}(\alpha_s/m_B^2, 1/m_B^3)$, where the second equation corresponds to a further use of $m_s = \mathcal{O}(\Lambda_{QCD})$. We get for the first two hadronic invariant mass moments [2]

$$\begin{aligned} \langle S_H \rangle &= m_s^2 + \bar{\Lambda}^2 + (m_B^2 - 2\bar{\Lambda} m_B) \langle \hat{s}_0 - \hat{m}_s^2 \rangle + (2\bar{\Lambda} m_B - 2\bar{\Lambda}^2 - \lambda_1 - 3\lambda_2) \langle x_0 \rangle \, , \\ \langle S_H^2 \rangle &= m_s^4 + 2\bar{\Lambda}^2 m_s^2 + 2m_s^2 (m_B^2 - 2\bar{\Lambda} m_B) \langle \hat{s}_0 - \hat{m}_s^2 \rangle + 2m_s^2 (2\bar{\Lambda} m_B - 2\bar{\Lambda}^2 - \lambda_1 - 3\lambda_2) \langle x_0 \rangle \\ &\quad + (m_B^4 - 4\bar{\Lambda} m_B^3) \langle (\hat{s}_0 - \hat{m}_s^2)^2 \rangle + 4\bar{\Lambda}^2 m_B^2 \langle x_0^2 \rangle + 4\bar{\Lambda} m_B^3 \langle x_0 (\hat{s}_0 - \hat{m}_s^2) \rangle \, , \qquad (62) \\ &= (m_B^4 - 4\bar{\Lambda} m_B^3) \langle (\hat{s}_0 - \hat{m}_s^2)^2 \rangle + 4\bar{\Lambda}^2 m_B^2 \langle x_0^2 \rangle + 4\bar{\Lambda} m_B^3 \langle x_0 (\hat{s}_0 - \hat{m}_s^2) \rangle \, , \end{aligned}$$

and for the hadron energy moments:

$$\begin{aligned} \langle E_H \rangle &= \bar{\Lambda} - \frac{\lambda_1 + 3\lambda_2}{2m_B} + \left(m_B - \bar{\Lambda} + \frac{\lambda_1 + 3\lambda_2}{2m_B} \right) \langle x_0 \rangle \, , \\ \langle E_H^2 \rangle &= \bar{\Lambda}^2 + (2\bar{\Lambda} m_B - 2\bar{\Lambda}^2 - \lambda_1 - 3\lambda_2) \langle x_0 \rangle \qquad (63) \\ &\quad + (m_B^2 - 2\bar{\Lambda} m_B + \bar{\Lambda}^2 + \lambda_1 + 3\lambda_2) \langle x_0^2 \rangle \, . \end{aligned}$$

One sees that there are linear power corrections, $\mathcal{O}(\bar{\Lambda}/m_B)$, present in all these hadronic quantities except $\langle S_H^2 \rangle$ which starts in $\frac{\alpha_s}{\pi} \frac{\bar{\Lambda}}{m_B}$.

5.1 Numerical Estimates of the Hadronic Moments in HQET

Using the expressions for the HQET moments given in appendix D, we present the numerical results for the hadronic moments in $B \to X_s \ell^+ \ell^-$, valid up to $\mathcal{O}(\alpha_s/m_B^2, 1/m_B^3)$. We find:

$$\langle x_0 \rangle = 0.367 \, (1 + 0.148 \frac{\alpha_s}{\pi} - 0.204 \frac{\bar{\Lambda}}{m_B} \frac{\alpha_s}{\pi} - 0.030 \frac{\bar{\Lambda}}{m_B} - 0.017 \frac{\bar{\Lambda}^2}{m_B^2} + 0.884 \frac{\lambda_1}{m_B^2} + 3.652 \frac{\lambda_2}{m_B^2}) \, ,$$

---

[2] Our first expression for $\langle S_H^2 \rangle$, eq. (62), does not agree in the coefficient of $\langle \hat{s}_0 - \hat{m}_s^2 \rangle$ with the one given in [32] (their eq. (4.1)). We point out that m_B^2 should have been replaced by m_b^2 in this expression. This has been confirmed by Adam Falk (private communication). Dropping the higher order terms given in their expressions, the hadronic moments in HQET derived here and in [32] agree.

$$\begin{aligned}
\langle x_0^2\rangle &= 0.147\,(1+0.324\frac{\alpha_s}{\pi}-0.221\frac{\bar\Lambda}{m_B}\frac{\alpha_s}{\pi}-0.058\frac{\bar\Lambda}{m_B}-0.034\frac{\bar\Lambda^2}{m_B^2}+1.206\frac{\lambda_1}{m_B^2}+4.680\frac{\lambda_2}{m_B^2})\,,\\
\langle x_0(\hat s_0-\hat m_s^2)\rangle &= 0.041\frac{\alpha_s}{\pi}(1+0.083\frac{\bar\Lambda}{m_B})+0.124\frac{\lambda_1}{m_B^2}+0.172\frac{\lambda_2}{m_B^2}\,,\\
\langle \hat s_0-\hat m_s^2\rangle &= 0.093\frac{\alpha_s}{\pi}(1+0.083\frac{\bar\Lambda}{m_B})+0.641\frac{\lambda_1}{m_B^2}+0.589\frac{\lambda_2}{m_B^2}\,,\\
\langle (\hat s_0-\hat m_s^2)^2\rangle &= 0.0071\frac{\alpha_s}{\pi}(1+0.083\frac{\bar\Lambda}{m_B})-0.196\frac{\lambda_1}{m_B^2}\,. \qquad (64)
\end{aligned}$$

As already discussed earlier, the normalizing factor $\mathcal{B}/\mathcal{B}_0$ is also expanded in a Taylor series. Thus, in deriving the above results, we have used

$$\frac{\mathcal{B}}{\mathcal{B}_0} = 25.277\ (1-1.108\frac{\alpha_s}{\pi}-0.083\frac{\bar\Lambda}{m_B}-0.041\frac{\bar\Lambda^2}{m_B^2}+0.546\frac{\lambda_1}{m_B^2}-3.439\frac{\lambda_2}{m_B^2})\,.$$

The parameters used in arriving at the numerical coefficients are given in Table 1 and Table 2.

Inserting the expressions for the moments calculated at the partonic level into eq. (62) and eq. (63), we find the following expressions for the short-distance hadronic moments, valid up to $\mathcal{O}(\alpha_s/m_B^2, 1/m_B^3)$:

$$\begin{aligned}
\langle S_H\rangle &= m_B^2(\frac{m_s^2}{m_B^2}+0.093\frac{\alpha_s}{\pi}-0.069\frac{\bar\Lambda}{m_B}\frac{\alpha_s}{\pi}+0.735\frac{\bar\Lambda}{m_B}+0.243\frac{\bar\Lambda^2}{m_B^2}+0.273\frac{\lambda_1}{m_B^2}-0.513\frac{\lambda_2}{m_B^2})\,,\\
\langle S_H^2\rangle &= m_B^4(0.0071\frac{\alpha_s}{\pi}+0.138\frac{\bar\Lambda}{m_B}\frac{\alpha_s}{\pi}+0.587\frac{\bar\Lambda^2}{m_B^2}-0.196\frac{\lambda_1}{m_B^2})\,, \qquad (65)\\
\langle E_H\rangle &= 0.367m_B(1+0.148\frac{\alpha_s}{\pi}-0.352\frac{\bar\Lambda}{m_B}\frac{\alpha_s}{\pi}+1.691\frac{\bar\Lambda}{m_B}+0.012\frac{\bar\Lambda^2}{m_B^2}+0.024\frac{\lambda_1}{m_B^2}+1.070\frac{\lambda_2}{m_B^2})\,,\\
\langle E_H^2\rangle &= 0.147m_B^2(1+0.324\frac{\alpha_s}{\pi}-0.128\frac{\bar\Lambda}{m_B}\frac{\alpha_s}{\pi}+2.954\frac{\bar\Lambda}{m_B}+2.740\frac{\bar\Lambda^2}{m_B^2}-0.299\frac{\lambda_1}{m_B^2}+0.162\frac{\lambda_2}{m_B^2})\,.
\end{aligned}$$

Setting $m_s=0$ changes the numerical value of the coefficients in the expansion given above (in which we already neglected $\alpha_s m_s$) by at most 1%. With the help of the expressions given above, we have calculated numerically the hadronic moments in HQET for the decay $B\to X_s\ell^+\ell^-$, $\ell=\mu,e$ and have estimated the errors by varying the parameters within their $\pm1\sigma$ ranges given in Table 1. They are presented in Table 3 where we have used $\bar\Lambda=0.39\,\mathrm{GeV}$, $\lambda_1=-0.2\,\mathrm{GeV}^2$ and $\lambda_2=0.12\,\mathrm{GeV}^2$. Further, using $\alpha_s(m_b)=0.21$, the explicit dependence of the hadronic moments given in eq. (65) on the HQET parameters λ_1 and $\bar\Lambda$ can be worked out:

$$\begin{aligned}
\langle S_H\rangle &= 0.0055m_B^2(1+132.61\frac{\bar\Lambda}{m_B}+44.14\frac{\bar\Lambda^2}{m_B^2}+49.66\frac{\lambda_1}{m_B^2})\,,\\
\langle S_H^2\rangle &= 0.00048m_B^4(1+19.41\frac{\bar\Lambda}{m_B}+1223.41\frac{\bar\Lambda^2}{m_B^2}-408.39\frac{\lambda_1}{m_B^2})\,, \qquad (66)\\
\langle E_H\rangle &= 0.372m_B(1+1.64\frac{\bar\Lambda}{m_B}+0.01\frac{\bar\Lambda^2}{m_B^2}+0.02\frac{\lambda_1}{m_B^2})\,,\\
\langle E_H^2\rangle &= 0.150m_B^2(1+2.88\frac{\bar\Lambda}{m_B}+2.68\frac{\bar\Lambda^2}{m_B^2}-0.29\frac{\lambda_1}{m_B^2})\,.
\end{aligned}$$

While interpreting these numbers, one should bear in mind that there are two comparable expansion parameters $\bar{\Lambda}/m_B$ and α_s/π and we have fixed the latter in showing the numbers. As expected, the dependence of the energy moments $\langle E_H^n \rangle$ on $\bar{\Lambda}$ and λ_1 is very weak. The correlations on the HQET parameters λ_1 and $\bar{\Lambda}$ which follow from (assumed) fixed values of the hadronic invariant mass moments $\langle S_H \rangle$ and $\langle S_H^2 \rangle$ are shown in Fig. 6. We have taken the values for the decay $B \to X_s \mu^+ \mu^-$ from Table 3 for the sake of illustration and have also shown the presently irreducible theoretical errors on these moments following from the input parameters m_t, α_s and the scale μ, given in Table 1. The errors were calculated by varying these parameters in the indicated range, one at a time, and adding the individual errors in quadrature. This exercise has to be repeated with real data in $B \to X_s \ell^+ \ell^-$to draw any quantitative conclusions.

The theoretical stability of the moments has to be checked against higher order corrections and the error estimates presented here will have to be improved. The "BLM-enhanced" two-loop corrections [44] proportional to $\alpha_s^2 \beta_0$, where $\beta_0 = 11 - 2n_f/3$ is the first term in the QCD beta function, can be included at the parton level as has been done in other decays [32,45], but not being crucial to our point we have not done this. More importantly, higher order corrections in α_s and $1/m_b^3$ are not included here. While we do not think that the higher orders in α_s will have a significant influence, the second moment $\langle S_H^2 \rangle$ is susceptible to the presence of $1/m_b^3$ corrections as shown for the decay $B \to X \ell \nu_\ell$ [46]. This will considerably enlarge the theoretical error represented by the dashed band for $\langle S_H^2 \rangle$ in Fig. 6. Fortunately, the coefficient of the $\bar{\Lambda}/m_B$ term in $\langle S_H \rangle$ is large. Hence, a good measurement of this moment alone constrains $\bar{\Lambda}$ effectively. Of course, the utility of the hadronic moments calculated above is only in conjunction with the experimental cuts. Since the optimal experimental cuts in $B \to X_s \ell^+ \ell^-$remain to be defined, we hope to return to this and related issue of doing an improved theoretical error estimate in a future publication.

Related issues in other decays have been studied in literature. The classification of the operators contributing in $\mathcal{O}(1/m_b^3)$, estimates of their matrix elements, and effects on the decay rates and spectra in the decays $B \to X \ell \nu_\ell$ and $B \to (D, D^*) \ell \nu_\ell$ have been studied in refs. [47–49]. Spectral moments of the photon energy in the decay $B \to X_s \gamma$ have been studied in ref. [50]. For studies of $\mathcal{O}(1/m_b^3)$ contributions in this decay and the effects of the experimental cut (on the photon energy) on the photon energy moments, see ref. [51].

Finally, concerning the power corrections related to the $c\bar{c}$ loop in $B \to X_s \ell^+ \ell^-$, it has been suggested in [20] that an $\mathcal{O}(\Lambda_{QCD}^2/m_c^2)$ expansion in the context of HQET can be carried out to take into account such effects in the invariant mass spectrum away from the resonances. Using the expressions (obtained with $m_s = 0$) for the $1/m_c^2$ amplitude, we have calculated the partonic energy

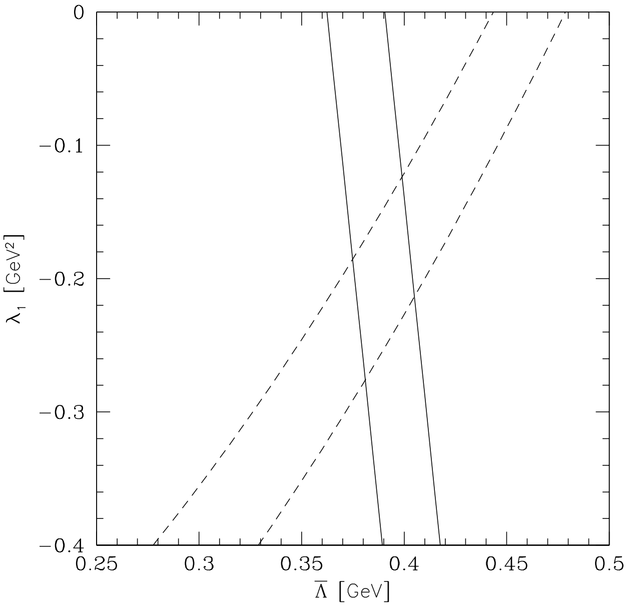

Figure 6: *$\langle S_H \rangle$ (solid bands) and $\langle S_H^2 \rangle$ (dashed bands) correlation in (λ_1-$\bar\Lambda$) space for fixed values $\langle S_H \rangle = 1.64\ GeV^2$ and $\langle S_H^2 \rangle = 4.48\ GeV^4$, corresponding to the central values in Table 3. The curves are forced to meet at the point $\lambda_1 = -0.2\ GeV^2$ and $\bar\Lambda = 0.39\ GeV$.*

HQET	$\langle S_H \rangle$	$\langle S_H^2 \rangle$	$\langle E_H \rangle$	$\langle E_H^2 \rangle$
	(GeV^2)	(GeV^4)	(GeV)	(GeV^2)
$\mu^+\mu^-$	1.64 ± 0.06	4.48 ± 0.29	2.21 ± 0.04	5.14 ± 0.16
e^+e^-	1.79 ± 0.07	4.98 ± 0.29	2.41 ± 0.06	6.09 ± 0.29

Table 3: *Hadronic spectral moments for $B \to X_s \mu^+\mu^-$ and $B \to X_s e^+e^-$ in HQET with $\bar\Lambda = 0.39\,GeV$, $\lambda_1 = -0.2\,GeV^2$, and $\lambda_2 = 0.12\,GeV^2$. The quoted errors result from varying μ, α_s and the top mass within the ranges given in Table 1.*

moments $\triangle\langle x_0^n \rangle$, which correct the short-distance result at order λ_2/m_c^2:

$$\begin{aligned} \triangle\langle x_0^n \rangle \frac{\mathcal{B}}{\mathcal{B}_0} &= -\frac{256 C_2 \lambda_2}{27 m_c^2} \int_0^{1/2(1-4\hat m_l^2)} dx_0 x_0^{n+2} \mathrm{Re}\left[F(r) \left(C_9^{\mathrm{eff}}(3-2x_0) + 2C_7^{\mathrm{eff}} \frac{-3+4x_0+2x_0^2}{2x_0-1} \right) \right] , \\ r &= \frac{1-2x_0}{4\hat m_c^2} , \end{aligned} \tag{67}$$

$$F(r) = \frac{3}{2r} \left\{ \begin{array}{ll} \frac{1}{\sqrt{r(1-r)}} \arctan\sqrt{\frac{r}{1-r}} - 1 & 0 < r < 1 , \\ \frac{1}{2\sqrt{r(r-1)}} \left(\ln \frac{1-\sqrt{1-1/r}}{1+\sqrt{1-1/r}} + i\pi \right) - 1 & r > 1 . \end{array} \right. \tag{68}$$

The invariant mass and mixed moments give zero contribution in the order we are working, with $m_s = 0$. Thus, the correction to the hadronic mass moments are vanishing, if we further neglect terms proportional to $\frac{\lambda_2}{m_c^2}\bar{\Lambda}$ and $\frac{\lambda_2}{m_c^2}\lambda_i$, with $i = 1, 2$. For the hadron energy moments we obtain numerically

$$\begin{aligned} \triangle\langle E_H\rangle_{1/m_c^2} &= m_B\triangle\langle x_0\rangle = -0.007\,\mathrm{GeV}\ , \\ \triangle\langle E_H^2\rangle_{1/m_c^2} &= m_B^2\triangle\langle x_0^2\rangle = -0.013\,\mathrm{GeV}^2\ , \end{aligned} \tag{69}$$

leading to a correction of order -0.3% to the short-distance values presented in Table 5. The power corrections presented here in the hadron spectrum and hadronic spectral moments in $B \to X_s\ell^+\ell^-$are the first results in this decay.

6 Hadron Spectra and Moments in the Fermi Motion Model

In this section, we study the non-perturbative effects associated with the bound state nature of the B hadron on the hadronic invariant mass and hadron energy distributions in the decay $B \to X_s\ell^+\ell^-$. These effects are studied in the FM model [28]. The hadronic moments in this model are compared with the ones calculated in the HQET approach for identical values of the equivalent parameters. We also define this equivalence and illustrate this numerically for some values of the FM model parameters resulting from fits of data in other B decays. With the help of the phenomenological profiles in the FM model, we study the effects of the experimental cuts used by the CLEO collaboration [30] on the hadron spectra and spectral moments in the decay $B \to X_s\ell^+\ell^-$. The resulting branching ratios and the hadronic invariant mass moments are calculated for several values of the FM parameters and can be compared directly with data when it becomes available.

6.1 Hadron spectra in $B \to X_s\ell^+\ell^-$ in the Fermi motion model [28]

The Fermi motion model [28] has received a lot of phenomenological attention in B decays, partly boosted by studies in the context of HQET showing that this model can be made to mimic the effects associated with the HQET parameters $\bar{\Lambda}$ and λ_1 [39,17]. We further quantify this correspondence in this paper. In the context of rare B decays, this model has been employed to calculate the energy spectra in the decay $B \to X_s + \gamma$ in [52], which was used subsequently by the CLEO collaboration in their successful search of this decay [53]. It has also been used in calculating the dilepton invariant mass spectrum and FB asymmetry in $B \to X_s\ell^+\ell^-$in ref. [15].

The FM model has two parameters p_F and the spectator quark mass m_q. Energy-momentum conservation requires the b-quark mass to be a momentum-dependent parameter determined by the constraint:

$$m_b^2(p) = {m_B}^2 + {m_q}^2 - 2m_B\sqrt{p^2 + {m_q}^2} \quad ; \quad p = |\vec{p}|\,. \tag{70}$$

The b-quark momentum p is assumed to have a Gaussian distribution, denoted by $\phi(p)$, which is determined by p_F

$$\phi(p) = \frac{4}{\sqrt{\pi} {p_F}^3} \exp(\frac{-p^2}{{p_F}^2}) \; , \tag{71}$$

with the normalization $\int_0^\infty dp\, p^2\, \phi(p) = 1$. In this model, the HQET parameters are calculable in terms of p_F and m_q with

$$\begin{aligned} \bar{\Lambda} &= \int_0^\infty dp\, p^2 \phi(p) \sqrt{m_q^2 + p^2}, \\ \lambda_1 &= -\int_0^\infty dp\, p^4 \phi(p) = -\frac{3}{2} p_F^2 \; . \end{aligned} \tag{72}$$

In addition, for $m_q = 0$, one can show that $\bar{\Lambda} = 2p_F/\sqrt{\pi}$. There is, however, no parameter in the FM model analogous to λ_2 in HQET. Curiously, much of the HQET *malaise* in describing the spectra in the end-point regions is related to λ_2, as also shown in [17,15]. For subsequent use in working out the normalization (decay widths) in the FM model, we also define an *effective* b-quark mass by

$$m_b^{\rm eff} \equiv (\int_0^\infty dp\, p^2\, m_b(p)^5 \phi(p))^{1/5} \; . \tag{73}$$

The relation between m_B, m_b, $\bar{\Lambda}$, λ_1 and λ_2 in HQET has already been stated. With the quantity $m_b^{\rm eff}$ defined in eq. (73) and the relations in eqs. (72) for λ_1 and $\bar{\Lambda}$, the relation

$$m_B = m_b^{\rm eff} + \bar{\Lambda} - \lambda_1/(2m_b^{\rm eff}) \; , \tag{74}$$

is found to be satisfied in the FM model to a high accuracy (better than 0.7%), which is shown in Table 4 for some representative values of the HQET parameters and their FM model equivalents. We shall use the HQET parameters $\bar{\Lambda}$ and λ_1 to characterize also the FM model parameters, with the relations given in eqs. (72) and (73) and in Table 4.

With this we turn to discuss the hadron energy spectrum in the decay $B \to X_s \ell^+ \ell^-$in the FM model including the $\mathcal{O}(\alpha_s)$ QCD corrections. The spectrum $\frac{{\rm d}\mathcal{B}}{{\rm d}E_H}(B \to X_s \ell^+ \ell^-)$ is composed of a Sudakov improved piece from C_9^2 and the remaining lowest order contribution. The latter is based on the parton model distribution, which is well known and given below for the sake of completeness:

$$\begin{aligned} \frac{{\rm d}\mathcal{B}}{{\rm d}s} &= \mathcal{B}_0 \frac{\bar{u}}{m_b^6} \left\{ \frac{4}{3} (m_b^4 - 2m_s^2 m_b^2 + m_s^4 + m_b^2 s + m_s^2 s - 2s^2) \left(|C_9^{\rm eff}(s)|^2 + |C_{10}|^2 \right) \right. \\ &+ \frac{16}{3} (2m_b^6 - 2m_b^4 m_s^2 - 2m_b^2 m_s^4 + 2m_s^6 - m_b^4 s - 14 m_b^2 m_s^2 s - m_s^4 s - m_b^2 s^2 - m_s^2 s^2) \frac{|C_7^{\rm eff}|^2}{s} \\ &+ \left. 16 (m_b^4 - 2m_s^2 m_b^2 + m_s^4 - m_b^2 s - m_s^2 s) Re(C_9^{\rm eff}(s))\, C_7^{\rm eff} \right\} \; , \end{aligned} \tag{75}$$

$$\begin{aligned} \bar{u} &= \frac{\sqrt{(m_b^2 + s - m_s^2)^2 - 4m_b^2 s}}{m_b^2} \; , \\ \mathcal{B}_0 &= \frac{\mathcal{B}_{sl}}{\Gamma_{sl}} \frac{G_F^2 |V_{ts}^* V_{tb}|^2}{192\pi^3} \frac{3\alpha^2}{16\pi^2} m_b^5 \; , \\ \Gamma_{sl} &= \frac{G_F^2 V_{cb}^2 m_b^5}{192\pi^3} f(\hat{m}_c) \kappa(\hat{m}_c) \; . \end{aligned} \tag{76}$$

Note that in the lowest order expression just given, we have $|C_9^{\rm eff}(s)|^2 = |Y(s)|^2 + 2C_9 Re(Y(s))$ with the rest of $C_9^{\rm eff}(s)$ now included in the Sudakov-improved piece as can be seen in eq. (32). To be consistent, the total semileptonic width Γ_{sl}, which enters via the normalization constant $\mathcal{B}_0$, has also to be calculated in the FM model with the same set of the model parameters. We implement the correction in the decay width by replacing the b-quark mass in Γ_{sl} given in eq. (76) by $m_b^{\rm eff}$. (See [15] for further quantitative discussions of this point on the branching ratio for the decay $B \to X_s \ell^+ \ell^-$.) The hadronic invariant mass spectrum in the decay $B \to X_s \ell^+ \ell^-$in this model is calculated very much along the same lines. The kinematically allowed ranges for the distributions are $m_X \leq E_H \leq m_B$ and $m_X^2 \leq S_H \leq m_B^2$, and we recall here that the physical threshold has been implemented by demanding that the lowest hadronic invariant mass produced in the decay $B \to X_s \ell^+ \ell^-$satisfies $m_X = max(m_K, m_q + m_s)$. The results for the hadron energy and the hadronic invariant mass spectra are presented in Figs. 7 and 9, respectively. We do not show the S_H distribution in the entire range, as it tends monotonically to zero for larger values of S_H.

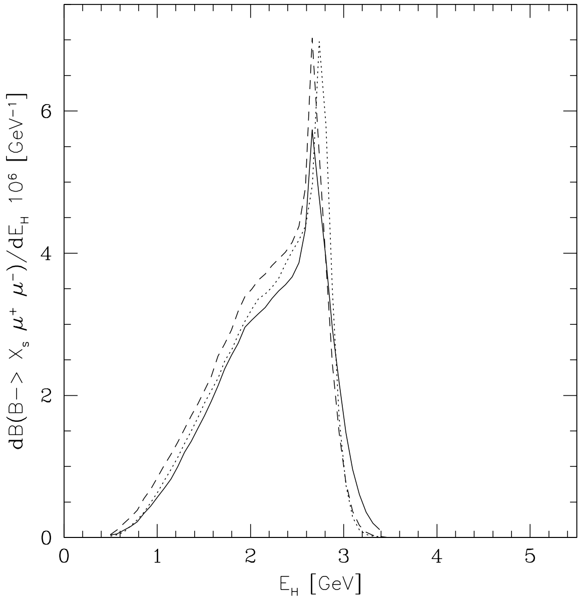

Figure 7: *Hadron energy spectrum in* $B \to X_s \ell^+ \ell^-$*in the Fermi motion model based on the perturbative contribution only. The solid, dotted, dashed curve corresponds to the parameters* $(\lambda_1, \bar{\Lambda}) = (-0.3, 0.5), (-0.1, 0.4), (-0.15, 0.35)$ *in (GeV*^{2}*, GeV), respectively.*

A number of remarks is in order:

- The hadron energy spectrum in $B \to X_s \ell^+ \ell^-$is rather insensitive to the model parameters. Also, the difference between the spectra in the FM and the parton model is rather small as can be seen in Fig. 8. Since, away from the lower end-point and the $c\bar{c}$ threshold, the parton model

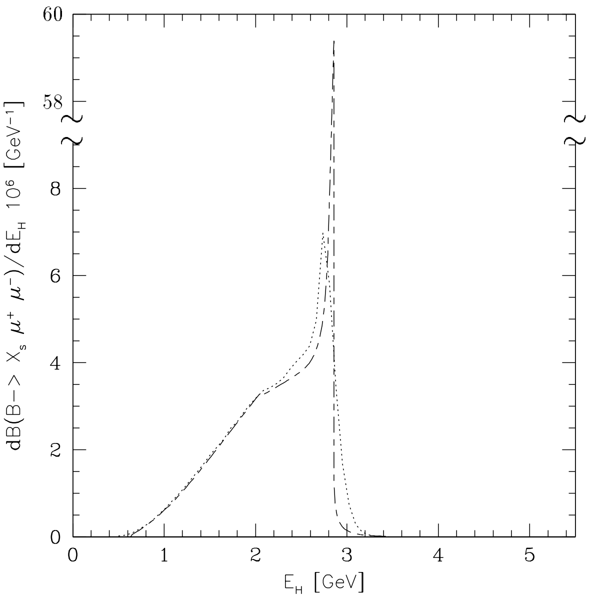

Figure 8: *Hadron energy spectrum in* $B \to X_s \ell^+ \ell^-$ *based on the perturbative contribution only, in the Fermi motion model (dotted curve) for* $(p_F, m_q) = (252, 300)$ (MeV, MeV), *yielding* $m_b^{eff} = 4.85$ *GeV, and in the parton model (long-short dashed curve) for* $m_b = 4.85$ *GeV.*

and HQET have very similar spectra (see Fig. 5), the estimates presented in Fig. 7 provide a good phenomenological profile of this spectrum for the short-distance contribution. Very similar conclusions were drawn in [33] for the corresponding spectrum in the decay $B \to X_u \ell \nu_\ell$, where, of course, the added complication of the $c\bar{c}$ threshold is not present.

- In contrast to the hadron energy spectrum, the hadronic invariant mass spectrum in $B \to X_s \ell^+ \ell^-$ is sensitive to the model parameters, as can be seen in Fig. 9. Again, one sees a close parallel in the hadronic invariant mass spectra in $B \to X_s \ell^+ \ell^-$ and $B \to X_u \ell \nu_\ell$, with the latter worked out in [34]. We think that the present theoretical dispersion on the hadron spectra in the decay $B \to X_s \ell^+ \ell^-$ can be considerably reduced by the analysis of data in $B \to X_u \ell \nu_\ell$.

- The hadronic invariant mass distribution obtained by the $O(\alpha_s)$-corrected partonic spectrum and the HQET mass relation can only be calculated over a limited range of S_H, $S_H > m_B \bar{\Lambda}$, as shown in Fig. 3. The larger is the value of $\bar{\Lambda}$, the smaller is this region. Also, in the range where it can be calculated, it depends on the non-perturbative parameter m_b (or $\bar{\Lambda}$). A comparison of this distribution and the one in the FM model may be made for the same values of m_b and $m_b^{\rm eff}$. This is shown for $m_b = 4.85$ GeV in Fig. 9 for HQET (long-short dashed curve) to be compared with the dotted curve in the FM model, which corresponds to $m_b^{\rm eff} = 4.85$ GeV. We see that the two distributions differ though they are qualitatively similar.

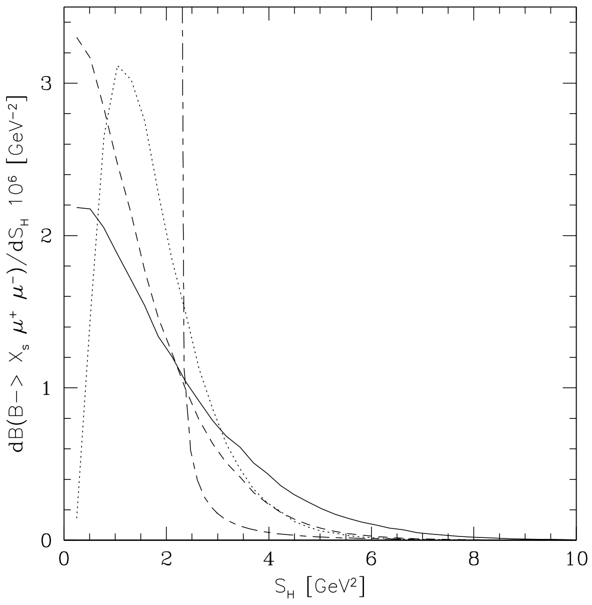

Figure 9: *Hadronic invariant mass spectrum in the Fermi motion model and parton model, based on the perturbative contribution only. The solid, dotted, dashed curve corresponds to the parameters* $(\lambda_1, \bar{\Lambda}) = (-0.3, 0.5), (-0.1, 0.4), (-0.15, 0.35)$ *in (GeV^2, GeV), respectively. The parton model (long-short dashed) curve is drawn for* $m_b = 4.85$ *GeV.*

6.2 Numerical Estimates of the Hadronic Moments in FM model and HQET

To underline the similarity of the HQET and FM descriptions in $B \to X_s \ell^+ \ell^-$, and also to make comparison with data when it becomes available with the FM model, we have calculated the hadronic moments in the FM model using the spectra just described. The moments are defined as usual:

$$\langle X_H^n \rangle \equiv (\int X_H^n \frac{d\mathcal{B}}{dX_H} dX_H)/\mathcal{B} \qquad \text{for} \quad X = S, E \, . \tag{77}$$

The values of the moments in both the HQET approach and the FM for $n = 1, 2$ are shown in Table 5 for the decay $B \to X_s \mu^+ \mu^-$, with the numbers in the parentheses corresponding to the former. They are based on using the central values of the parameters given in Table 1 and are calculated for the same values of the HQET parameters $\bar{\Lambda}$ and λ_1, using the transcriptions given in eqs. (72). Both the HQET and the FM model lead to strikingly similar results for the hadronic moments shown in this table. With $\langle S_H \rangle \simeq (1.5 - 2.1)$ GeV, the hadronic invariant mass spectra in $B \to X_s \ell^+ \ell^-$are expected to be dominated by multi-body states.

p_F, m_q (MeV,MeV)	$m_b^{\rm eff}$ (GeV)	λ_1 (GeV^2)	$\bar{\Lambda}$ (GeV)
$(450, 0)$	4.76	-0.304	0.507
$(252, 300)$	4.85	-0.095	0.422
$(310, 0)$	4.92	-0.144	0.350
$(450, 150)$	4.73	-0.304	0.534
$(500, 150)$	4.68	-0.375	0.588
$(570, 150)$	4.60	-0.487	0.664

Table 4: *Values of non perturbative parameters* m_b^{eff}*,* λ_1 *and* $\bar{\Lambda}$ *for different sets of the FM model parameters* (p_F, m_q) *taken from various fits of the data on* $B \to X_s + (J/\psi, \gamma)$ *decays discussed in ref. [29].*

	$\langle S_H \rangle$	$\langle S_H^2 \rangle$	$\langle E_H \rangle$	$\langle E_H^2 \rangle$
$(\lambda_1, \bar{\Lambda})$ in (GeV^2, GeV)	(GeV^2)	(GeV^4)	(GeV)	(GeV^2)
$(-0.3, 0.5)$	2.03 (2.09)	6.43 (6.93)	2.23 (2.28)	5.27 (5.46)
$(-0.1, 0.4)$	1.75 (1.80)	4.04 (4.38)	2.21 (2.22)	5.19 (5.23)
$(-0.14, 0.35)$	1.54 (1.49)	3.65 (3.64)	2.15 (2.18)	4.94 (5.04)

Table 5: *Hadronic spectral moments for* $B \to X_s \mu^+ \mu^-$ *in the Fermi motion model (HQET) for the indicated values of the parameters* $(\lambda_1, \bar{\Lambda})$*.*

7 Branching Ratios and Hadron Spectra in $B \to X_s \ell^+ \ell^-$ with Cuts on Invariant Masses

The short-distance (SD) contribution (electroweak penguins and boxes) is expected to be visible away from the resonance regions dominated by $B \to X_s (J/\psi, \psi', ...) \to X_s \ell^+ \ell^-$. So, cuts on the invariant dilepton mass are imposed to get quantitative control over the long-distance (LD) resonant contribution. For example, the cuts imposed in the recent CLEO analysis [30] given below are typical:

$$
\begin{aligned}
\text{cut A} &: \quad q^2 \leq (m_{J/\psi} - 0.1\,\text{GeV})^2 = 8.98\,\text{GeV}^2 \,, \\
\text{cut B} &: \quad q^2 \leq (m_{J/\psi} - 0.3\,\text{GeV})^2 = 7.82\,\text{GeV}^2 \,, \\
\text{cut C} &: \quad q^2 \geq (m_{\psi'} + 0.1\,\text{GeV})^2 = 14.33\,\text{GeV}^2 \,. \qquad (78)
\end{aligned}
$$

The cuts A and B have been chosen to take into account the QED radiative corrections as these effects are different in the e^+e^- and $\mu^+\mu^-$ modes. In a forthcoming paper [29], we shall compare the hadron spectra with and without the $B \to (J/\psi, \psi', ...) \to X_s \ell^+ \ell^-$ resonant parts after imposing these experimental cuts to quantify the theoretical uncertainty due to the residual LD-effects. Based on this study, we argue that the above cuts in q^2 greatly reduce the resonant part. Hence, the resulting distributions and moments with the above cuts essentially test (up to the non-perturbative aspects) the SD contribution in $B \to X_s \ell^+ \ell^-$.

As mentioned in [30], the dominant $B\bar{B}$ background to the decay $B \to X_s \ell^+ \ell^-$comes from two semileptonic decays of B or D mesons, which produce the lepton pair with two undetected neutrinos. To suppress this $B\bar{B}$ background, it is required that the invariant mass of the final hadronic state is less than $t = 1.8\,\text{GeV}$, which approximately equals m_D. We define the survival probability of the $B \to X_s \ell^+ \ell^-$signal after the hadronic invariant mass cut:

$$S(t) \equiv \left(\int_{m_X^2}^{t^2} \frac{d\mathcal{B}}{dS_H} dS_H\right)/\mathcal{B} \ , \tag{79}$$

and present $S(t = 1.8 \text{ GeV})$ as the fraction of the branching ratio for $B \to X_s \ell^+ \ell^-$surviving these cuts in Table 6. We note that the effect of this cut alone is that between 83% to 92% of the signal for $B \to X_s \mu^+ \mu^-$ and between 79% to 91% of the signal in $B \to X_s e^+ e^-$ survives, depending on the FM model parameters. This shows that while this cut removes a good fraction of the $B\bar{B}$ background, it allows a very large fraction of the $B \to X_s \ell^+ \ell^-$signal to survive. However, this cut does not discriminate between the SD- and LD- contributions, for which the cuts A - C are effective.

With the cut A (B) imposed on the dimuon (dielectron) invariant mass, we find that between 57% to 65% (57% to 68%) of the $B \to X_s \ell^+ \ell^-$signal survives the additional cut on the hadronic invariant mass for the SD contribution. The theoretical branching ratios for both the dielectron and dimuon cases, calculated using the central values in Table 1 are also given in Table 6. As estimated in [15], the uncertainty on the branching ratios resulting from the errors on the parameters in Table 1 is about ±28% (for the dielectron mode) and ±21% (for the dimuon case). The wave-function-related uncertainty in the branching ratios is negligible, as can be seen in Table 6. This reflects that, like in HQET, the corrections to the decay rates for $B \to X_s \ell^+ \ell^-$ and $B \to X \ell \nu_\ell$ are of order $1/m_b^2$, and a good part of these corrections cancel in the branching ratio for $B \to X_s \ell^+ \ell^-$. With the help of the theoretical branching ratios and the survival probability $S(t = 1.8 \text{ GeV})$, calculated for three sets of the FM parameters, the branching ratios can be calculated for all six cases with the indicated cuts in Table 6. This gives a fair estimate of the theoretical uncertainties on the partially integrated branching ratios from the B-meson wave function effects. This table shows that with 10^7 $B\bar{B}$ events, $\mathcal{O}(70)$ dimuon and $\mathcal{O}(100)$ dielectron signal events from $B \to X_s \ell^+ \ell^-$should survive the CLEO cuts A (B) with $m(X_s) < 1.8$ GeV. With cut C, one expects an order of magnitude less events, making this region interesting for the LHC experiments. We show in Fig. 10 hadron spectra in $B \to X_s \ell^+ \ell^-$, $\ell^\pm = e^\pm, \mu^\pm$, resulting after imposing the CLEO cuts A, B,C, defined in eq. (78). One sees that the general features of the (uncut) theoretical distributions remain largely intact: the hadron energy spectra are relatively insensitive to the FM parameters and the hadronic invariant mass spectra showing a sensitive dependence on them. Given enough data, one can compare the experimental distributions in $B \to X_s \ell^+ \ell^-$directly with the ones presented in Fig. 10.

FM parameters $(\lambda_1, \bar{\Lambda})$ in (GeV^2, GeV)	$\mathcal{B} \cdot 10^{-6}$ $\mu^+\mu^-$	$\mathcal{B} \cdot 10^{-6}$ e^+e^-	No s-cut $\mu^+\mu^-$	No s-cut e^+e^-	cut A $\mu^+\mu^-$	cut B e^+e^-	cut C $\mu^+\mu^-$	cut C e^+e^-
$(-0.3, 0.5)$	5.8	8.6	83%	79 %	57%	57%	6.4%	4.5%
$(-0.1, 0.4)$	5.7	8.4	93%	91 %	63%	68%	8.3%	5.8%
$(-0.14, 0.35)$	5.6	8.3	92%	90 %	65%	67%	7.9%	5.5%

Table 6: *Branching ratios for* $B \to X_s \ell^+ \ell^-$, $\ell = \mu, e$ *for different FM model parameters are given in the second and third columns. The values given in percentage in the fourth to ninth columns represent the survival probability* $S(t = 1.8 \text{ GeV})$, *defined in eq. (79), with no cut on the dilepton invariant mass and with cuts on this variable as defined in eq. (78).*

We have calculated the first two moments of the hadronic invariant mass in the FM model by imposing a cut $S_H < t^2$ with $t = 1.8\,\text{GeV}$ and an optional cut on q^2.

$$\langle S_H^n \rangle = \left(\int_{m_X^2}^{t^2} S_H^n \frac{d^2\mathcal{B}_{cutX}}{dS_H dq^2} dS_H dq^2\right) / \left(\int_{m_X^2}^{t^2} \frac{d^2\mathcal{B}_{cutX}}{dS_H dq^2} dS_H dq^2\right) \qquad \text{for} \quad n = 1, 2 \ . \tag{80}$$

Here the subscript *cutX* indicates whether we evaluated $\langle S_H \rangle$ and $\langle S_H^2 \rangle$ with the cuts on the invariant dilepton mass as defined in eq. (78), or without any cut on the dilepton mass. The results are collected in Table 7. The moments given in Table 7 can be compared directly with the data to extract the FM model parameters. The entries in this table give a fairly good idea of what the effects of the experimental cuts on the corresponding moments in HQET will be, as the FM and HQET yield very similar moments for equivalent values of the parameters. The functional dependence of the hadronic moments on the HQET parameters taking into account the experimental cuts still remains to be worked out.

FM parameters	No s-cut		No s-cut		cut A		cut B		cut C	
	$\mu^+\mu^-$		e^+e^-		$\mu^+\mu^-$		e^+e^-		$\ell^+\ell^-$	
$(\lambda_1, \bar{\Lambda})$	$\langle S_H \rangle$	$\langle S_H^2 \rangle$	$\langle S_H \rangle$	$\langle S_H^2 \rangle$	$\langle S_H \rangle$	$\langle S_H^2 \rangle$	$\langle S_H \rangle$	$\langle S_H^2 \rangle$	$\langle S_H \rangle$	$\langle S_H^2 \rangle$
GeV^2, GeV	GeV^2	GeV^4	GeV^2	GeV^4	GeV^2	GeV^4	GeV^2	GeV^4	GeV^2	GeV^4
$(-0.3, 0.5)$	1.47	2.87	1.52	3.05	1.62	3.37	1.66	3.48	0.74	0.69
$(-0.1, 0.4)$	1.57	2.98	1.69	3.37	1.80	3.71	1.88	3.99	0.74	0.63
$(-0.14, 0.35)$	1.31	2.34	1.38	2.55	1.47	2.83	1.52	2.97	0.66	0.54

Table 7: $\langle S_H \rangle$ *and* $\langle S_H^2 \rangle$ *for* $B \to X_s \ell^+ \ell^-$, $\ell = \mu, e$ *for different FM model parameters and a hadronic invariant mass cut* $S_H < 3.24\,GeV^2$ *are given in the second to fifth columns. The values in the sixth to eleventh columns have additional cuts on the dilepton invariant mass spectrum as defined in eq. (78). The* S_H*-moments with cuts are defined in eq. (80).*

8 Summary and Concluding Remarks

We summarize our results:

- We have calculated the $\mathcal{O}(\alpha_s)$ perturbative QCD and leading $\mathcal{O}(1/m_b)$ corrections to the hadron spectra in the decay $B \to X_s \ell^+ \ell^-$, including the Sudakov-improvements in the perturbative part.

- We find that the hadronic invariant mass spectrum is calculable in HQET over a limited range $S_H > m_B \bar{\Lambda}$ and it depends sensitively on the parameter $\bar{\Lambda}$ (equivalently m_b). These features are qualitatively very similar to the ones found for the hadronic invariant mass spectrum in the decay $B \to X_u \ell \nu_\ell$ [34].

- The $1/m_b$-corrections to the parton model hadron energy spectrum in $B \to X_s \ell^+ \ell^-$are small over most part of this spectrum. However, heavy quark expansion breaks down near the lower end-point of this spectrum and close to the $c\bar{c}$ threshold. The behavior in the former case has a similar origin as the breakdown of HQET near the high end-point in the dilepton invariant mass spectrum, found in ref. [15].

- We have calculated the hadronic spectral moments $\langle S_H^n \rangle$ and $\langle E_H^n \rangle$ for $n = 1, 2$ using HQET. The dependence of these moments on the HQET parameters is worked out numerically. In particular, the moments $\langle S_H^n \rangle$ are sensitive to the parameters $\bar{\Lambda}$ and λ_1 and they provide complementary constraints on them than the ones following from the analysis of the decay $B \to X \ell \nu_\ell$. The simultaneous fit of the data in $B \to X_s \ell^+ \ell^-$and $B \to X \ell \nu_\ell$ could then be used to determine these parameters very precisely. This has been illustrated in ref. [36] based on the present work.

- The corrections to the hadron energy moments $\triangle \langle E_H \rangle_{1/m_c^2}$ and $\triangle \langle E_H^2 \rangle_{1/m_c^2}$ from the leading $\mathcal{O}(\Lambda_{QCD}^2/m_c^2)$ power corrections have been worked out, using the results of ref. [20]. We find that these corrections are very small. The corresponding corrections in $\triangle \langle S_H^n \rangle_{1/m_c^2}$ vanish in the theoretical accuracy we are working.

- We think that the quantitative knowledge of $\bar{\Lambda}$ and λ_1 from the moments can be used to remove much of the theoretical uncertainties in the partially integrated decay rates in $B \to X_u \ell \nu_\ell$ and $B \to X_s \ell^+ \ell^-$. Realating the two decay rates would enable a precise determination of the CKM matrix element V_{ub}.

- As a phenomenological alternative to HQET, we have worked out the hadron spectra and spectral moments in $B \to X_s \ell^+ \ell^-$ in the Fermi motion model [28]. This complements the description of the final states in $B \to X_s \ell^+ \ell^-$presented in [15], where the dilepton invariant mass spectrum and FB asymmetry were worked out in both the HQET and FM model approaches. We find that the hadron energy spectrum is stable against the variation of the FM model parameters. However, the hadronic invariant mass is sensitive to the input parameters. For equivalent values of the FM and HQET parameters, the spectral moments are found to be remarkably close to each other.

- We have worked out the hadron spectra and spectral moments in the FM model by imposing the CLEO experimental cuts designed to suppress the resonant $c\bar{c}$ contributions, as well as the dominant $B\bar{B}$ background leading to the final state $B\bar{B} \to X_s \ell^+ \ell^-$ (+ missing energy). The parametric dependence of the resulting spectra is studied. In particular, the survival probability of the $B \to X_s \ell^+ \ell^-$ signal is estimated by imposing a cut on the hadronic invariant mass $S_H < 3.24$ GeV^2 and on the dilepton invariant mass as used in the CLEO analysis. The spectra and moments can be directly compared with data.

We hope that the work presented here will contribute to precise determinations of the HQET parameters and V_{ub} using the inclusive decays $B \to X_s \ell^+ \ell^-$ and $B \to X_u \ell \nu_\ell$ in forthcoming B facilities.

Acknowledgements

We would like to thank Tomasz Skwarnicki for drawing our attention to the importance of the hadron spectra in the search for the decay $B \to X_s \ell^+ \ell^-$. We thank Christoph Greub for helpful discussions. Correspondence with Adam Falk and Gino Isidori on power corrections are thankfully acknowledged.

Appendices

A Coefficient Functions $g_i^{(9,10)}, g_i^{(7)}, g_i^{(7,9)}, h_i^{(9)}, h_i^{(7,9)}, k_1^{(9)}, k_1^{(7,9)}$

These functions enter in the derivation of the leading $(1/m_b^2)$ corrections to the hadron energy spectrum in $B \to X_s \ell^+ \ell^-$, given in eq. (53).

$$
\begin{aligned}
g_0^{(9,10)} &= \sqrt{x_0^2 - \hat{m}_s^2}\frac{32}{3}(-2\hat{m}_s^2 + 3x_0 + 3\hat{m}_s^2 x_0 - 4x_0^2) \,, && \text{(A-1)}\\
g_1^{(9,10)} &= \frac{1}{\sqrt{x_0^2 - \hat{m}_s^2}}\frac{16}{9}(9\hat{m}_s^2 + 23\hat{m}_s^4 - 18\hat{m}_s^2 x_0 - 18x_0^2 - 52\hat{m}_s^2 x_0^2 + 36x_0^3 + 20x_0^4) \,, && \text{(A-2)}\\
g_2^{(9,10)} &= \frac{1}{\sqrt{x_0^2 - \hat{m}_s^2}}\frac{16}{3}(3\hat{m}_s^2 + 23\hat{m}_s^4 - 3x_0 - 21\hat{m}_s^2 x_0 - 6x_0^2 - 52\hat{m}_s^2 x_0^2 + 36x_0^3 + 20x_0^4) \,, && \text{(A-3)}\\
g_0^{(7)} &= \sqrt{x_0^2 - \hat{m}_s^2}\frac{64}{3}(10\hat{m}_s^2 + 10\hat{m}_s^4 - 3x_0 - 18\hat{m}_s^2 x_0 - 3\hat{m}_s^4 x_0 + 2x_0^2 + 2\hat{m}_s^2 x_0^2) \,, && \text{(A-4)}\\
g_1^{(7)} &= \frac{1}{\sqrt{x_0^2 - \hat{m}_s^2}}\frac{1}{(x_0 - \frac{1}{2}(1+\hat{m}_s^2))^2}\frac{-8}{9}(9\hat{m}_s^2 + 34\hat{m}_s^4 + 104\hat{m}_s^6 + 110\hat{m}_s^8 + 31\hat{m}_s^{10} - 132\hat{m}_s^4 x_0 - 312\hat{m}_s^6 x_0 \\
&- 180\hat{m}_s^8 x_0 - 18x_0^2 - 170\hat{m}_s^2 x_0^2 - 58\hat{m}_s^4 x_0^2 + 74\hat{m}_s^6 x_0^2 - 20\hat{m}_s^8 x_0^2 + 72x_0^3 + 564\hat{m}_s^2 x_0^3 + 576\hat{m}_s^4 x_0^3 \\
&+ 228\hat{m}_s^6 x_0^3 - 116x_0^4 - 676\hat{m}_s^2 x_0^4 - 436\hat{m}_s^4 x_0^4 - 20\hat{m}_s^6 x_0^4 + 72x_0^5 + 240\hat{m}_s^2 x_0^5 + 24\hat{m}_s^4 x_0^5) \,, && \text{(A-5)}\\
g_2^{(7)} &= \frac{1}{\sqrt{x_0^2 - \hat{m}_s^2}}\frac{1}{x_0 - \frac{1}{2}(1+\hat{m}_s^2)}\frac{16}{3}(27\hat{m}_s^2 + 93\hat{m}_s^4 + 97\hat{m}_s^6 + 31\hat{m}_s^8 - 3x_0 - 63\hat{m}_s^2 x_0 - 189\hat{m}_s^4 x_0 \\
&- 129\hat{m}_s^6 x_0 - 18x_0^2 - 108\hat{m}_s^2 x_0^2 - 62\hat{m}_s^4 x_0^2 - 20\hat{m}_s^6 x_0^2 + 72x_0^3 + 324\hat{m}_s^2 x_0^3 + 180\hat{m}_s^4 x_0^3 - 60x_0^4 \\
&- 152\hat{m}_s^2 x_0^4 - 20\hat{m}_s^4 x_0^4) \,, && \text{(A-6)}\\
g_0^{(7,9)} &= \sqrt{x_0^2 - \hat{m}_s^2}128(-2\hat{m}_s^2 + x_0 + \hat{m}_s^2 x_0) \,, && \text{(A-7)}\\
g_1^{(7,9)} &= \frac{1}{\sqrt{x_0^2 - \hat{m}_s^2}}64(\hat{m}_s^2 + 3\hat{m}_s^4 + 2\hat{m}_s^2 x_0 - 2x_0^2 - 4\hat{m}_s^2 x_0^2) \,, && \text{(A-8)}\\
g_2^{(7,9)} &= \frac{1}{\sqrt{x_0^2 - \hat{m}_s^2}}64(5\hat{m}_s^2 + 9\hat{m}_s^4 - x_0 + 5\hat{m}_s^2 x_0 - 6x_0^2 - 12\hat{m}_s^2 x_0^2) \,, && \text{(A-9)}\\
h_1^{(9,10)} &= \frac{32}{9}\sqrt{x_0^2 - \hat{m}_s^2}(-12\hat{m}_s^2 - 6\hat{m}_s^4 + 9x_0 + 19\hat{m}_s^2 x_0 + 3x_0^2 + 15\hat{m}_s^2 x_0^2 - 28x_0^3) \,, && \text{(A-10)}\\
h_2^{(9,10)} &= \frac{32}{3}\sqrt{x_0^2 - \hat{m}_s^2}(-6\hat{m}_s^4 + 3x_0 + 5\hat{m}_s^2 x_0 + 3x_0^2 + 15\hat{m}_s^2 x_0^2 - 20x_0^3) \,, && \text{(A-11)}\\
h_1^{(7,9)} &= \frac{128}{3}\sqrt{x_0^2 - \hat{m}_s^2}(-8\hat{m}_s^2 - 2\hat{m}_s^4 + 3x_0 - 3\hat{m}_s^2 x_0 + 5x_0^2 + 5\hat{m}_s^2 x_0^2) \,, && \text{(A-12)}\\
h_2^{(7,9)} &= \frac{128}{3}\sqrt{x_0^2 - \hat{m}_s^2}(-4\hat{m}_s^2 - 6\hat{m}_s^4 + 3x_0 - 15\hat{m}_s^2 x_0 + 7x_0^2 + 15\hat{m}_s^2 x_0^2) \,, && \text{(A-13)}\\
k_1^{(9,10)} &= \frac{64}{9}\sqrt{x_0^2 - \hat{m}_s^2}^{\,3}(2\hat{m}_s^2 - 3x_0 - 3\hat{m}_s^2 x_0 + 4x_0^2) \,, && \text{(A-14)}\\
k_1^{(7,9)} &= \frac{-256}{3}\sqrt{x_0^2 - \hat{m}_s^2}^{\,3}(-2\hat{m}_s^2 + x_0 + \hat{m}_s^2 x_0) \,. && \text{(A-15)}
\end{aligned}
$$

B Auxiliary Functions $f_\delta(\hat{\lambda}_1, \hat{\lambda}_2), f_{\delta'}(\hat{\lambda}_1, \hat{\lambda}_2)$

The auxiliary functions given below are the coefficients of the singular terms in the derivation of the leading $(1/m_b^2)$ corrections to the hadron energy spectrum in $B \to X_s \ell^+ \ell^-$, given in eq. (53).

$$
\begin{aligned}
f_\delta(\hat{\lambda}_1, \hat{\lambda}_2) \;=\;& \mathcal{B}_0 \Bigg\{ \Bigg[\frac{2}{9}(1-\hat{m}_s^2)^3(5-\hat{m}_s^2)\hat{\lambda}_1 \\
+\;& \frac{2}{3}(1-\hat{m}_s^2)^3(-1+5\hat{m}_s^2)\hat{\lambda}_2 \Bigg] \left(|C_9^{\text{eff}}|^2 + |C_{10}|^2 \right) \\
+\;& \Bigg[\frac{1}{9}(1 + 12\hat{m}_l^2 - 88\hat{m}_l^4 - 4\hat{m}_s^2 - 36\hat{m}_l^2\hat{m}_s^2 - 736\hat{m}_l^4\hat{m}_s^2 + 5\hat{m}_s^4 + 24\hat{m}_l^2\hat{m}_s^4 + 720\hat{m}_l^4\hat{m}_s^4 \\
+\;& 24\hat{m}_l^2\hat{m}_s^6 + 160\hat{m}_l^4\hat{m}_s^6 - 5\hat{m}_s^8 - 36\hat{m}_l^2\hat{m}_s^8 - 56\hat{m}_l^4\hat{m}_s^8)\frac{\hat{\lambda}_1}{\hat{m}_l^2} + \frac{4}{3}(-1+\hat{m}_s^2)(-3 \\
+\;& 14\hat{m}_l^2 - 2\hat{m}_s^2 + 166\hat{m}_l^2\hat{m}_s^2 + 8\hat{m}_s^4 + 154\hat{m}_l^2\hat{m}_s^4 + 2\hat{m}_s^6 + 50\hat{m}_l^2\hat{m}_s^6 - 5\hat{m}_s^8)\hat{\lambda}_2 \Bigg] \frac{|C_7^{\text{eff}}|^2}{\hat{m}_l^2} \\
+\;& \Bigg[\frac{8}{3}(1-\hat{m}_s^2)^3(7+\hat{m}_s^2)\hat{\lambda}_1 + \frac{8}{3}(1-\hat{m}_s^2)^3(13+15\hat{m}_s^2)\hat{\lambda}_2 \Bigg] Re(C_9^{\text{eff}})\, C_7^{\text{eff}} \\
+\;& \hat{\lambda}_1(-1+\hat{m}_s^2)^5 \Big(\frac{2}{9}\frac{d|C_9^{\text{eff}}|^2}{d\hat{s}_0} + \frac{8}{3}\frac{dRe(C_9^{\text{eff}})}{d\hat{s}_0}\, C_7^{\text{eff}} \Big) \Bigg\} . \qquad \text{(B-16)}
\end{aligned}
$$

$$
\begin{aligned}
f_{\delta'}(\hat{\lambda}_1, \hat{\lambda}_2) \;=\;& \mathcal{B}_0 \hat{\lambda}_1 \Bigg\{ \frac{1}{9}(1-\hat{m}_s^2)^5 \left(|C_9^{\text{eff}}|^2 + |C_{10}|^2 \right) \\
+\;& \frac{2}{9}(-1+\hat{m}_s^2)^3(-1 + 14\hat{m}_l^2 + \hat{m}_s^2 + 52\hat{m}_l^2\hat{m}_s^2 + \hat{m}_s^4 + 14\hat{m}_l^2\hat{m}_s^4 - \hat{m}_s^6)\frac{|C_7^{\text{eff}}|^2}{\hat{m}_l^2} \\
+\;& \frac{4}{3}(1-\hat{m}_s^2)^5 Re(C_9^{\text{eff}})\, C_7^{\text{eff}} \Bigg\} . \qquad \text{(B-17)}
\end{aligned}
$$

C The Functions $\alpha_i, \beta_i, \gamma_i, \delta_i$

The functions entering in the definition of the hadron moments in eq. (57) are given in this appendix. Note that the functions $\alpha_i^{(n,m)}$ and $\beta_i^{(n,m)}$ multiply the Wilson coefficients $|C_7^{\text{eff}}|^2$ and C_{10}^2, respectively. Their results are given in a closed form. The functions $\gamma_i^{(n,m)}$ multiply the Wilson coefficients $C_7^{\text{eff}} Re(C_9^{\text{eff}})$, of which $Re(C_9^{\text{eff}})$ is an implicit function of x_0. Likewise, the functions $\delta_i^{(n,m)}$ multiply the Wilson coefficient $|C_9^{\text{eff}}|^2$. The expressions for $\gamma_i^{(n,m)}$ and $\delta_i^{(n,m)}$ are given in the form of one-dimensional integrals over x_0.

The functions $\alpha_i^{(n,m)}$

$$
\begin{aligned}
\alpha_0^{(0,0)} \;=\;& \frac{16}{9}(-8 - 26\hat{m}_s^2 + 18\hat{m}_s^4 + 22\hat{m}_s^6 - 11\hat{m}_s^8) + \frac{32}{3}(-1+\hat{m}_s^2)^3(1+\hat{m}_s^2)\ln(4\hat{m}_l^2) \\
+\;& \frac{64}{3}\hat{m}_s^4(-9 - 2\hat{m}_s^2 + \hat{m}_s^4)\ln(\hat{m}_s)\;, \qquad \text{(C-18)} \\
\alpha_1^{(0,0)} \;=\;& \frac{1}{2}\alpha_0^{(0,0)}\;, \qquad \text{(C-19)} \\
\alpha_2^{(0,0)} \;=\;& \frac{8}{3}(-4 + 38\hat{m}_s^2 - 42\hat{m}_s^4 - 26\hat{m}_s^6 - 15\hat{m}_s^8) + 16(-1+\hat{m}_s^2)^2(3 + 8\hat{m}_s^2 + 5\hat{m}_s^4)\ln(4\hat{m}_l^2)
\end{aligned}
$$

$$+ \quad 32\hat{m}_s^2(-8-17\hat{m}_s^2-2\hat{m}_s^4+5\hat{m}_s^6)\ln(\hat{m}_s)\ , \tag{C-20}$$

$$\begin{aligned}\alpha_0^{(0,1)} &= \frac{2}{9}(-41-49\hat{m}_s^2+256\hat{m}_s^4-128\hat{m}_s^6-43\hat{m}_s^8)+\frac{16}{3}(-1+\hat{m}_s^2)^3(1+\hat{m}_s^2)^2\ln(4\hat{m}_l^2)\\ &+ \frac{16}{3}\hat{m}_s^4(3-\hat{m}_s^2-2\hat{m}_s^4)\ln(\hat{m}_s)\ ,\end{aligned} \tag{C-21}$$

$$\alpha_1^{(0,1)} = \alpha_1^{(0,0)}\ , \tag{C-22}$$

$$\begin{aligned}\alpha_2^{(0,1)} &= \frac{4}{9}(21+167\hat{m}_s^2+128\hat{m}_s^4-276\hat{m}_s^6-319\hat{m}_s^8)+\frac{16}{3}(-1+\hat{m}_s^2)^2(3+14\hat{m}_s^2+21\hat{m}_s^4+10\hat{m}_s^6)\ln(4\hat{m}_l^2)\\ &+ \frac{32}{3}\hat{m}_s^2(3-24\hat{m}_s^2-18\hat{m}_s^4+\hat{m}_s^6)\ln(\hat{m}_s)\ ,\end{aligned} \tag{C-23}$$

$$\begin{aligned}\alpha_0^{(0,2)} &= \frac{2}{45}(-119-144\hat{m}_s^2+45\hat{m}_s^4+320\hat{m}_s^6+45\hat{m}_s^8)+\frac{8}{3}(-1+\hat{m}_s^4)^3\ln(4\hat{m}_l^2)\\ &- \frac{16}{3}\hat{m}_s^6(8+3\hat{m}_s^2)\ln(\hat{m}_s)\ ,\end{aligned} \tag{C-24}$$

$$\begin{aligned}\alpha_1^{(0,2)} &= \frac{1}{27}(-127-278\hat{m}_s^2+1075\hat{m}_s^4-800\hat{m}_s^6+49\hat{m}_s^8)+\frac{4}{9}(1-\hat{m}_s^2)^3(-7-17\hat{m}_s^2-5\hat{m}_s^4+5\hat{m}_s^6)\ln(4\hat{m}_l^2)\\ &+ \frac{8}{9}\hat{m}_s^4(18-38\hat{m}_s^2-13\hat{m}_s^4)\ln(\hat{m}_s)\ ,\end{aligned} \tag{C-25}$$

$$\begin{aligned}\alpha_2^{(0,2)} &= \frac{1}{9}(27-46\hat{m}_s^2+1681\hat{m}_s^4-688\hat{m}_s^6-1189\hat{m}_s^8)+\frac{4}{3}(-1+\hat{m}_s^4)^2(3+20\hat{m}_s^2+25\hat{m}_s^4)\ln(4\hat{m}_l^2)\\ &- \frac{8}{3}\hat{m}_s^4(18+54\hat{m}_s^2+47\hat{m}_s^4)\ln(\hat{m}_s)\ ,\end{aligned} \tag{C-26}$$

$$\alpha_0^{(1,0)} = 0\ , \tag{C-27}$$

$$\begin{aligned}\alpha_1^{(1,0)} &= \frac{2}{9}(-23-159\hat{m}_s^2-112\hat{m}_s^4+304\hat{m}_s^6-45\hat{m}_s^8)-\frac{16}{3}(-1+\hat{m}_s^2)^4(1+\hat{m}_s^2)\ln(4\hat{m}_l^2)\\ &+ \frac{16}{3}\hat{m}_s^4(-39-7\hat{m}_s^2+6\hat{m}_s^4)\ln(\hat{m}_s)\ ,\end{aligned} \tag{C-28}$$

$$\begin{aligned}\alpha_2^{(1,0)} &= \frac{2}{9}(-93-469\hat{m}_s^2+704\hat{m}_s^4-127\hat{m}_s^8)+\frac{16}{3}(-1+\hat{m}_s^2)^3(3+8\hat{m}_s^2+5\hat{m}_s^4)\ln(4\hat{m}_l^2)\\ &- \frac{112}{3}\hat{m}_s^4(3+3\hat{m}_s^2+2\hat{m}_s^4)\ln(\hat{m}_s)\ ,\end{aligned} \tag{C-29}$$

$$\alpha_0^{(1,1)} = 0\ , \tag{C-30}$$

$$\begin{aligned}\alpha_1^{(1,1)} &= \frac{2}{27}(-4-131\hat{m}_s^2+307\hat{m}_s^4-416\hat{m}_s^6+178\hat{m}_s^8)-\frac{8}{9}(-1+\hat{m}_s^2)^4(1+6\hat{m}_s^2+5\hat{m}_s^4)\ln(4\hat{m}_l^2)\\ &+ \frac{16}{9}\hat{m}_s^4(9-35\hat{m}_s^2-7\hat{m}_s^4)\ln(\hat{m}_s)\ ,\end{aligned} \tag{C-31}$$

$$\begin{aligned}\alpha_2^{(1,1)} &= \frac{2}{9}(-60-185\hat{m}_s^2+173\hat{m}_s^4+160\hat{m}_s^6+70\hat{m}_s^8)+\frac{8}{3}(-1+\hat{m}_s^2)^3(1+\hat{m}_s^2)^2(3+5\hat{m}_s^2)\ln(4\hat{m}_l^2)\\ &+ \frac{16}{3}\hat{m}_s^4(3-21\hat{m}_s^2-13\hat{m}_s^4)\ln(\hat{m}_s)\ ,\end{aligned} \tag{C-32}$$

$$\alpha_0^{(2,0)} = 0\ , \tag{C-33}$$

$$\begin{aligned}\alpha_1^{(2,0)} &= \frac{8}{135}(119-176\hat{m}_s^2-1085\hat{m}_s^4+400\hat{m}_s^6+835\hat{m}_s^8)+\frac{32}{9}(1-\hat{m}_s^2)^5(1+\hat{m}_s^2)\ln(4\hat{m}_l^2)\\ &- \frac{64}{9}\hat{m}_s^6(28+5\hat{m}_s^2)\ln(\hat{m}_s)\ ,\end{aligned} \tag{C-34}$$

$$\alpha_2^{(2,0)} = 0\,. \tag{C-35}$$

The functions $\beta_i^{(n,m)}$

$$\beta_0^{(0,0)} = \frac{2}{3}(1-8\hat{m}_s^2+8\hat{m}_s^6-\hat{m}_s^8-24\hat{m}_s^4\ln(\hat{m}_s))\ , \tag{C-36}$$

$$\beta_1^{(0,0)} = \frac{1}{2}\beta_0^{(0,0)} , \tag{C-37}$$

$$\beta_2^{(0,0)} = -3 + 8\hat{m}_s^2 - 24\hat{m}_s^4 + 24\hat{m}_s^6 - 5\hat{m}_s^8 - 24\hat{m}_s^4 \ln(\hat{m}_s) , \tag{C-38}$$

$$\beta_0^{(0,1)} = \frac{1}{30}(7 - 25\hat{m}_s^2 + 160\hat{m}_s^4 - 160\hat{m}_s^6 + 25\hat{m}_s^8 - 7\hat{m}_s^{10} + 120\hat{m}_s^4 \ln(\hat{m}_s) + 120\hat{m}_s^6 \ln(\hat{m}_s)) , \tag{C-39}$$

$$\beta_1^{(0,1)} = \beta_1^{(0,0)} , \tag{C-40}$$

$$\beta_2^{(0,1)} = \frac{1}{3}\hat{m}_s^2(7 - 20\hat{m}_s^2 + 20\hat{m}_s^6 - 7\hat{m}_s^8 + 24\ln(\hat{m}_s) - 48\hat{m}_s^2 \ln(\hat{m}_s)) , \tag{C-41}$$

$$\beta_0^{(0,2)} = \frac{2}{45}(2 - 3\hat{m}_s^2 - 30\hat{m}_s^4 + 30\hat{m}_s^8 + 3\hat{m}_s^{10} - 2\hat{m}_s^{12} - 120\hat{m}_s^6 \ln(\hat{m}_s)) , \tag{C-42}$$

$$\begin{aligned}\beta_1^{(0,2)} &= \frac{1}{270}(43 - 135\hat{m}_s^2 + 1260\hat{m}_s^4 - 1440\hat{m}_s^6 + 405\hat{m}_s^8 - 153\hat{m}_s^{10} + 20\hat{m}_s^{12} + 1080\hat{m}_s^4 \ln(\hat{m}_s) \\ &+ 840\hat{m}_s^6 \ln(\hat{m}_s)) ,\end{aligned} \tag{C-43}$$

$$\begin{aligned}\beta_2^{(0,2)} &= \frac{1}{90}(13 - 315\hat{m}_s^2 + 1500\hat{m}_s^4 - 1560\hat{m}_s^6 + 315\hat{m}_s^8 + 147\hat{m}_s^{10} - 100\hat{m}_s^{12} + 360\hat{m}_s^4 \ln(\hat{m}_s) \\ &+ 840\hat{m}_s^6 \ln(\hat{m}_s)) ,\end{aligned} \tag{C-44}$$

$$\beta_0^{(1,0)} = 0 , \tag{C-45}$$

$$\beta_1^{(1,0)} = \frac{1}{30}(13 - 135\hat{m}_s^2 - 160\hat{m}_s^4 + 320\hat{m}_s^6 - 45\hat{m}_s^8 + 7\hat{m}_s^{10} - 600\hat{m}_s^4 \ln(\hat{m}_s) - 120\hat{m}_s^6 \ln(\hat{m}_s)) , \tag{C-46}$$

$$\beta_2^{(1,0)} = \frac{1}{6}(3 - 9\hat{m}_s^2 + 16\hat{m}_s^4 - 48\hat{m}_s^6 + 45\hat{m}_s^8 - 7\hat{m}_s^{10} + 24\hat{m}_s^4 \ln(\hat{m}_s) - 72\hat{m}_s^6 \ln(\hat{m}_s)) , \tag{C-47}$$

$$\beta_0^{(1,1)} = 0 , \tag{C-48}$$

$$\begin{aligned}\beta_1^{(1,1)} &= \frac{1}{270}(23 - 45\hat{m}_s^2 + 1080\hat{m}_s^4 - 1440\hat{m}_s^6 + 585\hat{m}_s^8 - 243\hat{m}_s^{10} + 40\hat{m}_s^{12} + 1080\hat{m}_s^4 \ln(\hat{m}_s) \\ &+ 600\hat{m}_s^6 \ln(\hat{m}_s)) ,\end{aligned} \tag{C-49}$$

$$\beta_2^{(1,1)} = \frac{1}{90}(13 + 45\hat{m}_s^2 - 120\hat{m}_s^4 - 45\hat{m}_s^8 + 147\hat{m}_s^{10} - 40\hat{m}_s^{12} + 360\hat{m}_s^4 \ln(\hat{m}_s) - 600\hat{m}_s^6 \ln(\hat{m}_s)) , \tag{C-50}$$

$$\beta_0^{(2,0)} = 0 , \tag{C-51}$$

$$\beta_1^{(2,0)} = \frac{16}{135}(-1 + 9\hat{m}_s^2 - 45\hat{m}_s^4 + 45\hat{m}_s^8 - 9\hat{m}_s^{10} + \hat{m}_s^{12} - 120\hat{m}_s^6 \ln(\hat{m}_s)) , \tag{C-52}$$

$$\beta_2^{(2,0)} = 0 . \tag{C-53}$$

The functions $\gamma_i^{(n,m)}$

Note that in the expressions given below $C_9^{\rm eff} \equiv C_9^{\rm eff}(\hat{s} = 1 - 2x_0 + \hat{m}_s^2)$. The lower and upper limits of the x_0-integrals are: $x_0^{min} = \hat{m}_s$ and $x_0^{max} = \frac{1}{2}(1 + \hat{m}_s^2 - 4\hat{m}_l^2)$.

$$\gamma_0^{(0,0)} = 128 \int_{x_0^{min}}^{x_0^{max}} dx_0 \sqrt{x_0^2 - \hat{m}_s^2}(-2\hat{m}_s^2 + x_0 + \hat{m}_s^2 x_0) Re(C_9^{\rm eff}) , \tag{C-54}$$

$$\gamma_1^{(0,0)} = \frac{1}{2}\gamma_0^{(0,0)} , \tag{C-55}$$

$$\begin{aligned}\gamma_2^{(0,0)} &= \int_{x_0^{min}}^{x_0^{max}} dx_0 \frac{64}{\sqrt{x_0^2 - \hat{m}_s^2}}(4\hat{m}_s^2 + 14\hat{m}_s^4 - x_0 - \hat{m}_s^2 x_0 - 12\hat{m}_s^4 x_0 - 4x_0^2 - 22\hat{m}_s^2 x_0^2 + 7x_0^3 \\ &+ 15\hat{m}_s^2 x_0^3) Re(C_9^{\rm eff}) ,\end{aligned} \tag{C-56}$$

$$\gamma_0^{(0,1)} = 128 \int_{x_0^{min}}^{x_0^{max}} dx_0 x_0 \sqrt{x_0^2 - \hat{m}_s^2}(-2\hat{m}_s^2 + x_0 + \hat{m}_s^2 x_0) Re(C_9^{\rm eff}) , \tag{C-57}$$

$$\gamma_1^{(0,1)} = \gamma_1^{(0,0)} \, , \tag{C-58}$$

$$\begin{aligned} \gamma_2^{(0,1)} &= \frac{64}{3}\int_{x_0^{min}}^{x_0^{max}} dx_0 \frac{1}{\sqrt{x_0^2-\hat{m}_s^2}}(4\hat{m}_s^4 + 6\hat{m}_s^6 + 9\hat{m}_s^2 x_0 + 57\hat{m}_s^4 x_0 - 3x_0^2 - 14\hat{m}_s^2 x_0^2 - 57\hat{m}_s^4 x_0^2 \\ &- 9x_0^3 - 81\hat{m}_s^2 x_0^3 + 28x_0^4 + 60\hat{m}_s^2 x_0^4) Re(C_9^{\rm eff}) \, , \end{aligned} \tag{C-59}$$

$$\gamma_0^{(0,2)} = 128\int_{x_0^{min}}^{x_0^{max}} dx_0 x_0^2 \sqrt{x_0^2-\hat{m}_s^2}(-2\hat{m}_s^2 + x_0 + \hat{m}_s^2 x_0) Re(C_9^{\rm eff}) \, , \tag{C-60}$$

$$\begin{aligned} \gamma_1^{(0,2)} &= \frac{64}{3}\int_{x_0^{min}}^{x_0^{max}} dx_0 \sqrt{x_0^2-\hat{m}_s^2}(-4\hat{m}_s^4 - 10\hat{m}_s^2 x_0 + 2\hat{m}_s^4 x_0 + 6x_0^2 + 16\hat{m}_s^2 x_0^2 - 5x_0^3 \\ &- 5\hat{m}_s^2 x_0^3) Re(C_9^{\rm eff}) \, , \end{aligned} \tag{C-61}$$

$$\begin{aligned} \gamma_2^{(0,2)} &= \frac{64}{3}\int_{x_0^{min}}^{x_0^{max}} dx_0 \frac{x_0}{\sqrt{x_0^2-\hat{m}_s^2}}(8\hat{m}_s^4 + 12\hat{m}_s^6 + 6\hat{m}_s^2 x_0 + 72\hat{m}_s^4 x_0 - 3x_0^2 - 25\hat{m}_s^2 x_0^2 - 78\hat{m}_s^4 x_0^2 \\ &- 6x_0^3 - 96\hat{m}_s^2 x_0^3 + 35x_0^4 + 75\hat{m}_s^2 x_0^4) Re(C_9^{\rm eff}) \, , \end{aligned} \tag{C-62}$$

$$\gamma_0^{(1,0)} = 0 \, , \tag{C-63}$$

$$\gamma_1^{(1,0)} = 128\int_{x_0^{min}}^{x_0^{max}} dx_0 \frac{(x_0-1)}{\sqrt{x_0^2-\hat{m}_s^2}}(-2\hat{m}_s^4 + \hat{m}_s^2 x_0 + \hat{m}_s^4 x_0 + 2\hat{m}_s^2 x_0^2 - x_0^3 - \hat{m}_s^2 x_0^3) Re(C_9^{\rm eff}) \, , \tag{C-64}$$

$$\gamma_2^{(1,0)} = \frac{128}{3}\int_{x_0^{min}}^{x_0^{max}} dx_0 \sqrt{x_0^2-\hat{m}_s^2}(-4\hat{m}_s^2 - 6\hat{m}_s^4 + 3x_0 - 15\hat{m}_s^2 x_0 + 7x_0^2 + 15\hat{m}_s^2 x_0^2) Re(C_9^{\rm eff}) \, , \tag{C-65}$$

$$\gamma_0^{(1,1)} = 0 \, , \tag{C-66}$$

$$\begin{aligned} \gamma_1^{(1,1)} &= \frac{128}{3}\int_{x_0^{min}}^{x_0^{max}} dx_0 \frac{1}{\sqrt{x_0^2-\hat{m}_s^2}}(4\hat{m}_s^6 + 4\hat{m}_s^4 x_0 - 2\hat{m}_s^6 x_0 - 3\hat{m}_s^2 x_0^2 - 17\hat{m}_s^4 x_0^2 + \hat{m}_s^2 x_0^3 + 7\hat{m}_s^4 x_0^3 \\ &+ 3x_0^4 + 13\hat{m}_s^2 x_0^4 - 5x_0^5 - 5\hat{m}_s^2 x_0^5) Re(C_9^{\rm eff}) \, , \end{aligned} \tag{C-67}$$

$$\gamma_2^{(1,1)} = \frac{128}{3}\int_{x_0^{min}}^{x_0^{max}} dx_0 x_0 \sqrt{x_0^2-\hat{m}_s^2}(-4\hat{m}_s^2 - 6\hat{m}_s^4 + 3x_0 - 15\hat{m}_s^2 x_0 + 7x_0^2 + 15\hat{m}_s^2 x_0^2) Re(C_9^{\rm eff}) \, , \tag{C-68}$$

$$\gamma_0^{(2,0)} = 0 \, , \tag{C-69}$$

$$\gamma_1^{(2,0)} = \frac{512}{3}\int_{x_0^{min}}^{x_0^{max}} dx_0 \sqrt{x_0^2-\hat{m}_s^2}(-2\hat{m}_s^4 + \hat{m}_s^2 x_0 + \hat{m}_s^4 x_0 + 2\hat{m}_s^2 x_0^2 - x_0^3 - \hat{m}_s^2 x_0^3) Re(C_9^{\rm eff}) \, , \tag{C-70}$$

$$\gamma_2^{(2,0)} = 0 \, . \tag{C-71}$$

The functions $\delta_i^{(n,m)}$

$$\delta_0^{(0,0)} = \frac{32}{3}\int_{x_0^{min}}^{x_0^{max}} dx_0 \sqrt{x_0^2-\hat{m}_s^2}(-2\hat{m}_s^2 + 3x_0 + 3\hat{m}_s^2 x_0 - 4x_0^2)|C_9^{\rm eff}|^2 \, , \tag{C-72}$$

$$\delta_1^{(0,0)} = \frac{1}{2}\delta_0^{(0,0)} \, , \tag{C-73}$$

$$\begin{aligned} \delta_2^{(0,0)} &= \int_{x_0^{min}}^{x_0^{max}} dx_0 \frac{16}{\sqrt{x_0^2-\hat{m}_s^2}}(6\hat{m}_s^4 - x_0 - 9\hat{m}_s^2 x_0 - 12\hat{m}_s^4 x_0 + 6\hat{m}_s^2 x_0^2 + 15x_0^3 + 15\hat{m}_s^2 x_0^3 \\ &- 20x_0^4)|C_9^{\rm eff}|^2 \, , \end{aligned} \tag{C-74}$$

$$\delta_0^{(0,1)} = \frac{32}{3}\int_{x_0^{min}}^{x_0^{max}} dx_0 x_0 \sqrt{x_0^2-\hat{m}_s^2}(-2\hat{m}_s^2 + 3x_0 + 3\hat{m}_s^2 x_0 - 4x_0^2)|C_9^{\rm eff}|^2 \, , \tag{C-75}$$

$$\delta_1^{(0,1)} = \delta_1^{(0,0)} \, , \tag{C-76}$$

$$\begin{aligned}
\delta_2^{(0,1)} &= \frac{16}{3}\int_{x_0^{min}}^{x_0^{max}} dx_0 \frac{1}{\sqrt{x_0^2-\hat{m}_s^2}}(6\hat{m}_s^6-3\hat{m}_s^2x_0+13\hat{m}_s^4x_0-3x_0^2-30\hat{m}_s^2x_0^2-57\hat{m}_s^4x_0^2+3x_0^3 \\
&+ 43\hat{m}_s^2x_0^3+48x_0^4+60\hat{m}_s^2x_0^4-80x_0^5)|C_9^{\rm eff}|^2\ , \qquad \text{(C-77)} \\
\delta_0^{(0,2)} &= \frac{32}{3}\int_{x_0^{min}}^{x_0^{max}} dx_0 x_0^2\sqrt{x_0^2-\hat{m}_s^2}(-2\hat{m}_s^2+3x_0+3\hat{m}_s^2x_0-4x_0^2)|C_9^{\rm eff}|^2\ , \qquad \text{(C-78)} \\
\delta_1^{(0,2)} &= \frac{16}{9}\int_{x_0^{min}}^{x_0^{max}} dx_0 \sqrt{x_0^2-\hat{m}_s^2}(-4\hat{m}_s^4-6\hat{m}_s^2x_0+6\hat{m}_s^4x_0+18x_0^2+20\hat{m}_s^2x_0^2-39x_0^3-15\hat{m}_s^2x_0^3 \\
&+ 20x_0^4)|C_9^{\rm eff}|^2\ , \qquad \text{(C-79)} \\
\delta_2^{(0,2)} &= \frac{16}{3}\int_{x_0^{min}}^{x_0^{max}} dx_0 \frac{x_0}{\sqrt{x_0^2-\hat{m}_s^2}}(12\hat{m}_s^6-6\hat{m}_s^2x_0+8\hat{m}_s^4x_0-3x_0^2-33\hat{m}_s^2x_0^2-78\hat{m}_s^4x_0^2+6x_0^3 \\
&+ 68\hat{m}_s^2x_0^3+51x_0^4+75\hat{m}_s^2x_0^4-100x_0^5)|C_9^{\rm eff}|^2\ , \qquad \text{(C-80)} \\
\delta_0^{(1,0)} &= 0\ , \qquad \text{(C-81)} \\
\delta_1^{(1,0)} &= \frac{32}{3}\int_{x_0^{min}}^{x_0^{max}} dx_0 \frac{(x_0-1)}{\sqrt{x_0^2-\hat{m}_s^2}}(-2\hat{m}_s^4+3\hat{m}_s^2x_0+3\hat{m}_s^4x_0-2\hat{m}_s^2x_0^2-3x_0^3-3\hat{m}_s^2x_0^3+4x_0^4)|C_9^{\rm eff}|^2\ , \text{(C-82)} \\
\delta_2^{(1,0)} &= \frac{32}{3}\int_{x_0^{min}}^{x_0^{max}} dx_0 \sqrt{x_0^2-\hat{m}_s^2}(-6\hat{m}_s^4+3x_0+5\hat{m}_s^2x_0+3x_0^2+15\hat{m}_s^2x_0^2-20x_0^3)|C_9^{\rm eff}|^2\ , \qquad \text{(C-83)} \\
\delta_0^{(1,1)} &= 0\ , \qquad \text{(C-84)} \\
\delta_1^{(1,1)} &= \frac{32}{9}\int_{x_0^{min}}^{x_0^{max}} dx_0 \frac{1}{\sqrt{x_0^2-\hat{m}_s^2}}(4\hat{m}_s^6-6\hat{m}_s^6x_0-9\hat{m}_s^2x_0^2-15\hat{m}_s^4x_0^2+27\hat{m}_s^2x_0^3+21\hat{m}_s^4x_0^3 \\
&+ 9x_0^4-9\hat{m}_s^2x_0^4-27x_0^5-15\hat{m}_s^2x_0^5+20x_0^6)|C_9^{\rm eff}|^2\ , \qquad \text{(C-85)} \\
\delta_2^{(1,1)} &= \frac{32}{3}\int_{x_0^{min}}^{x_0^{max}} dx_0 x_0\sqrt{x_0^2-\hat{m}_s^2}(-6\hat{m}_s^4+3x_0+5\hat{m}_s^2x_0+3x_0^2+15\hat{m}_s^2x_0^2-20x_0^3)|C_9^{\rm eff}|^2\ , \qquad \text{(C-86)} \\
\delta_0^{(2,0)} &= 0\ , \qquad \text{(C-87)} \\
\delta_1^{(2,0)} &= \frac{128}{9}\int_{x_0^{min}}^{x_0^{max}} dx_0 \sqrt{x_0^2-\hat{m}_s^2}(-2\hat{m}_s^4+3\hat{m}_s^2x_0+3\hat{m}_s^4x_0-2\hat{m}_s^2x_0^2-3x_0^3 \\
&- 3\hat{m}_s^2x_0^3+4x_0^4)|C_9^{\rm eff}|^2\ , \qquad \text{(C-88)} \\
\delta_2^{(2,0)} &= 0\ . \qquad \text{(C-89)}
\end{aligned}$$

D Lowest Hadronic Moments (Parton Level)

$$\begin{aligned}
\langle x_0\rangle\frac{\mathcal{B}}{\mathcal{B}_0} &= \frac{2}{9m_B^2}(-41m_B^2-49m_s^2-24(m_B^2-m_s^2)\ln(4\frac{m_l^2}{m_B^2}))C_7^{\rm eff^2}+\frac{1}{30m_B^2}(7m_B^2-25m_s^2)C_{10}^2 \\
&+ \int_{m_s/m_B}^{\frac{1}{2}(1+m_s^2/m_B^2)} dx_0\frac{64}{m_B^2}x_0(-m_s^2-4m_s^2x_0+2m_B^2x_0^2+2m_s^2x_0^2)Re(C_9^{\rm eff})C_7^{\rm eff} \\
&+ \int_{m_s/m_B}^{\frac{1}{2}(1+m_s^2/m_B^2)} dx_0\frac{16}{3m_B^2}x_0(-3m_s^2+6m_B^2x_0^2+6m_s^2x_0^2-8m_B^2x_0^3)|C_9^{\rm eff}|^2 \\
&+ \frac{\alpha_s}{\pi}A^{(0,1)}C_9^2+\frac{-32}{3}C_7^{\rm eff^2}\frac{\bar{\Lambda}}{m_B}+\frac{-16}{3}C_7^{\rm eff^2}\frac{\bar{\Lambda}^2}{m_B^2}+\Bigg[\frac{-16}{9}(1+3\ln(4\frac{m_l^2}{m_B^2}))C_7^{\rm eff^2}+\frac{C_{10}^2}{3}
\end{aligned}$$

$$\begin{aligned}
&+ \int_0^{\frac{1}{2}} dx_0 (64 x_0^2 Re(C_9^{\mathrm{eff}}) C_7^{\mathrm{eff}} + \frac{16}{3}(3 - 4x_0) x_0^2 |C_9^{\mathrm{eff}}|^2)\Bigg] \frac{\lambda_1}{m_B^2} \\
&+ \Bigg[\frac{4}{3}(19 + 12\ln(4\frac{m_l^2}{m_B^2}))C_7^{\mathrm{eff}2} + \int_0^{\frac{1}{2}} dx_0 (\frac{64}{3} x_0(-3 - 9x_0 + 28x_0^2) Re(C_9^{\mathrm{eff}}) C_7^{\mathrm{eff}} \\
&+ \frac{16}{3} x_0(-3 + 3x_0 + 48x_0^2 - 80x_0^3)|C_9^{\mathrm{eff}}|^2\Bigg] \frac{\lambda_2}{m_B^2}\,,
\end{aligned}\tag{D-90}$$

$$\begin{aligned}
\langle x_0^2\rangle \frac{\mathcal{B}}{\mathcal{B}_0} &= \frac{2}{45 m_B^{12}}(-119 m_B^{12} - 144 m_B^{10} m_s^2 - 60(m_B^{12} - m_s^{12})\ln(4\frac{m_l^2}{m_B^2}))C_7^{\mathrm{eff}2} + \frac{2}{45 m_B^2}(2m_B^2 - 3m_s^2)C_{10}^2 \\
&+ \int_{m_s/m_B}^{\frac{1}{2}(1+m_s^2/m_B^2)} dx_0 \frac{64}{m_B^2} x_0^2(-m_s^2 - 4m_s^2 x_0 + 2m_B^2 x_0^2 + 2m_s^2 x_0^2) Re(C_9^{\mathrm{eff}}) C_7^{\mathrm{eff}} \\
&+ \int_{m_s/m_B}^{\frac{1}{2}(1+m_s^2/m_B^2)} dx_0 \frac{16}{3m_B^2} x_0^2(-3m_s^2 + 6m_B^2 x_0^2 + 6m_s^2 x_0^2 - 8m_B^2 x_0^3)|C_9^{\mathrm{eff}}|^2 \\
&+ \frac{\alpha_s}{\pi} A^{(0,2)} C_9^2 + \frac{-16}{3} C_7^{\mathrm{eff}2} \frac{\bar{\Lambda}}{m_B} + \frac{-8}{3} C_7^{\mathrm{eff}2} \frac{\bar{\Lambda}^2}{m_B^2} + \Bigg[\frac{-1}{27}(55 + 84\ln(4\frac{m_l^2}{m_B^2}))C_7^{\mathrm{eff}2} + 43\frac{C_{10}^2}{270} \\
&+ \int_0^{\frac{1}{2}} dx_0 (\frac{64}{3}(6 - 5x_0) x_0^3 Re(C_9^{\mathrm{eff}}) C_7^{\mathrm{eff}} + \frac{16}{9}(18 - 39x_0 + 20x_0^2) x_0^3 |C_9^{\mathrm{eff}}|^2)\Bigg] \frac{\lambda_1}{m_B^2} \\
&+ \Bigg[(11 + 4\ln(4\frac{m_l^2}{m_B^2}))C_7^{\mathrm{eff}2} + 13\frac{C_{10}^2}{90} + \int_0^{\frac{1}{2}} dx_0 (\frac{64}{3} x_0^2(-3 - 6x_0 + 35x_0^2) Re(C_9^{\mathrm{eff}}) C_7^{\mathrm{eff}} \\
&+ \frac{16}{3} x_0^2(-3 + 6x_0 + 51x_0^2 - 100x_0^3)|C_9^{\mathrm{eff}}|^2\Bigg] \frac{\lambda_2}{m_B^2}\,,
\end{aligned}\tag{D-91}$$

$$\begin{aligned}
\langle x_0(\hat{s}_0 - \hat{m}_s^2)\rangle \frac{\mathcal{B}}{\mathcal{B}_0} &= \frac{\alpha_s}{\pi} A^{(1,1)} C_9^2 + \Bigg[\frac{-8}{27}(1 + 3\ln(4\frac{m_l^2}{m_B^2}))C_7^{\mathrm{eff}2} + 23\frac{C_{10}^2}{270} \\
&+ \int_0^{\frac{1}{2}} dx_0 (\frac{128}{3}(3 - 5x_0) x_0^3 Re(C_9^{\mathrm{eff}}) C_7^{\mathrm{eff}} + \frac{32}{9}(9 - 27x_0 + 20x_0^2) x_0^3 |C_9^{\mathrm{eff}}|^2)\Bigg] \frac{\lambda_1}{m_B^2} \\
&+ \Bigg[\frac{-8}{3}(5 + 3\ln(4\frac{m_l^2}{m_B^2}))C_7^{\mathrm{eff}2} + 13\frac{C_{10}^2}{90} \\
&+ \int_0^{\frac{1}{2}} dx_0 (\frac{128}{3} x_0^3(3 + 7x_0) Re(C_9^{\mathrm{eff}}) C_7^{\mathrm{eff}} + \frac{32}{3} x_0^3(3 + 3x_0 - 20x_0^2)|C_9^{\mathrm{eff}}|^2\Bigg] \frac{\lambda_2}{m_B^2}\,,
\end{aligned}\tag{D-92}$$

$$\begin{aligned}
\langle \hat{s}_0 - \hat{m}_s^2\rangle \frac{\mathcal{B}}{\mathcal{B}_0} &= \frac{\alpha_s}{\pi} A^{(1,0)} C_9^2 + \Bigg[\frac{-2}{9}(23 + 24\ln(4\frac{m_l^2}{m_B^2}))C_7^{\mathrm{eff}2} + 13\frac{C_{10}^2}{30} \\
&+ \int_0^{\frac{1}{2}} dx_0 (128(1 - x_0) x_0^2 Re(C_9^{\mathrm{eff}}) C_7^{\mathrm{eff}} + \frac{32}{3}(3 - 7x_0 + 4x_0^2) x_0^2 |C_9^{\mathrm{eff}}|^2)\Bigg] \frac{\lambda_1}{m_B^2} \\
&+ \Bigg[\frac{-2}{3}(31 + 24\ln(4\frac{m_l^2}{m_B^2}))C_7^{\mathrm{eff}2} + \frac{C_{10}^2}{2} \\
&+ \int_0^{\frac{1}{2}} dx_0 (\frac{128}{3} x_0^2(3 + 7x_0) Re(C_9^{\mathrm{eff}}) C_7^{\mathrm{eff}} + \frac{32}{3} x_0^2(3 + 3x_0 - 20x_0^2)|C_9^{\mathrm{eff}}|^2\Bigg] \frac{\lambda_2}{m_B^2}\,,
\end{aligned}\tag{D-93}$$

$$\begin{aligned}
\langle(\hat{s}_0 - \hat{m}_s^2)^2\rangle \frac{\mathcal{B}}{\mathcal{B}_0} &= \frac{\alpha_s}{\pi} A^{(2,0)} C_9^2 + \Bigg[\frac{8}{135}(119 + 60\ln(4\frac{m_l^2}{m_B^2}))C_7^{\mathrm{eff}2} - 16\frac{C_{10}^2}{135} \\
&+ \int_0^{\frac{1}{2}} dx_0 (\frac{-512}{3} x_0^4 Re(C_9^{\mathrm{eff}}) C_7^{\mathrm{eff}} + \frac{128}{9}(-3 + 4x_0) x_0^4 |C_9^{\mathrm{eff}}|^2)\Bigg] \frac{\lambda_1}{m_B^2}\,.
\end{aligned}\tag{D-94}$$

References

[1] T. Skwarnicki, preprint HEPSY 97-03, hep-ph/9712253; to be published in Proc. of the Seventh Int. Symp. on Heavy Flavor Physics, UC Santa Barbara, California, July 7-11, 1997.

[2] A. Ali, preprint DESY 97-256, hep-ph/9801270; to be published in Proc. of the First APCTP Workshop, Pacific Particle Physics Phenomenology, Seoul, South Korea, Oct. 31 - Nov. 2, 1997.

[3] W.S. Hou, R.I. Willey and A. Soni, Phys. Rev. Lett. **58**, 1608 (1987).

[4] B. Grinstein, M.J. Savage and M.B. Wise, Nucl. Phys. **319**, 271 (1989).

[5] W. Jaus and D. Wyler, Phys. Rev. **D41**, 3405 (1990).

[6] R. M. Barnett et al., Review of Particle Properties, Phys. Rev. **54**, 1 (1996).

[7] S. Bertolini, F. Borzumati, A. Masiero and R. Ridolfi, Nucl. Phys. **B353**, 591 (1991).

[8] A. Ali, G.F. Giudice and T. Mannel, Z. Phys. **C67**, 417 (1995).

[9] P. Cho, M. Misiak and D. Wyler, Phys. Rev. **D54**, 3329 (1996).

[10] T. Goto, Y. Okada, Y. Shimizu and M. Tanaka, Phys. Rev. **D55**, 4273 (1997).

[11] J.L. Hewett and J. Wells, Phys. Rev. **D55**, 55 (1997).

[12] A. J. Buras and M. Münz, Phys. Rev. **D52**, 186 (1995).

[13] M. Misiak, Nucl. Phys. **B393**, 23 (1993) [E. **B439**, 461 (1995)].

[14] A. Ali, T. Mannel and T. Morozumi, Phys. Lett. **B273**, 505 (1991).

[15] A. Ali, L. T. Handoko, G. Hiller and T. Morozumi, Phys. Rev. **D55**, 4105 (1997).

[16] J. Chay, H. Georgi and B. Grinstein, Phys. Lett. **B247**, 399 (1990); I.I. Bigi, N.G. Uraltsev and A.I. Vainshtein, Phys. Lett. **B293**, 430 (1992) [E. **B297**, 477 (1993)]; I.I. Bigi et al., Phys. Rev. Lett. **71**, 496 (1993); B. Blok et al., Phys. Rev. **D49**, 3356 (1994) [E. **D50**, 3572 (1994)].

[17] A. Manohar and M. B. Wise, Phys. Rev. **D49**, 1310 (1994).

[18] A. F. Falk, M. Luke and M. J. Savage, Phys. Rev. **D49**, 3367 (1994).

[19] G. Buchalla and G. Isidori, preprint CERN-TH/97-374, LNF-98/003(P), hep-ph/9801456.

[20] G. Buchalla, G. Isidori and S. -J. -Rey, Nucl. Phys. **B511**, 594 (1998).

[21] J.-W. Chen, G. Rupak and M. J. Savage, Phys. Lett. **B410**, 285 (1997).

[22] M.B. Voloshin, Phys. Lett. **B397**, 275 (1997).

[23] A. Khodjamirian et al., Phys. Lett. **B402**, 167 (1997); Z. Ligeti, L. Randall and M.B. Wise, Phys. Lett. **B402**, 178 (1997); A.K. Grant et al., Phys. Rev. **D56**, 3151 (1997).

[24] D.S. Liu and R. Delbourgo, Phys. Rev. **D55**, 7044 (1997).

[25] O. Bär and N. Pott, Phys. Rev. **D55**, 1684 (1997).

[26] J.L. Hewett, Phys. Rev. **D53**, 4964 (1996).

[27] F. Krüger and L.M. Sehgal, Phys. Lett. **B380**, 199 (1996).

[28] A. Ali and E. Pietarinen, Nucl. Phys. **B154**, 519 (1979);
G. Altarelli et al., Nucl. Phys. **B208**, 365 (1982).

[29] A. Ali and G. Hiller, DESY Report 98-031.

[30] S. Glenn et al. (CLEO Collaboration), Phys. Rev. Lett. **80**, 2289 (1998).

[31] V. Barger, C.S. Kim and R.J.N. Philips, Phys. Lett. **B251**, 629 (1990).

[32] A. F. Falk, M. Luke and M. J. Savage, Phys. Rev. **D53**, 2491 (1996).

[33] C. Greub and S.-J. Rey, Phys. Rev. **D56**, 4250 (1997).

[34] A.F. Falk, Z. Ligeti and M.B. Wise, Phys. Lett. **B406**, 225 (1997).

[35] R.D. Dikeman and N.G. Uraltsev, Nucl. Phys. **B509**, 378 (1998); see also, I.I. Bigi, R.D. Dikeman and N.G. Uraltsev, preprint TPI-MINN-97-21, hep-ph/9706520.

[36] A. Ali and G. Hiller, DESY Report 98-025, hep-ph/9803407 (submitted to Physical Review Letters).

[37] M. Gremm, A. Kapustin, Z. Ligeti and M.B. Wise, Phys. Rev. Lett. **77**, 20 (1996).

[38] M. Neubert, preprint CERN-TH/98-2, hep-ph/9801269; to be published in Proc. of the Int. Europhys. Conf. on High Energy Physics, Jerusalem, Israel, 19 - 26 August, 1997.

[39] I.I. Bigi et al., Phys. Lett. **B328**, 431 (1994).

[40] A. Czarnecki, M. Jeżabek and J. H. Kühn, Acta. Phys. Pol. **B20**, 961 (1989);
M. Jeżabek and J. H. Kühn, Nucl. Phys. **B320**, 20 (1989).

[41] A. Ali, Z. Phys. **C1**, 25 (1979).

[42] N. Cabibbo and L. Maiani, Phys. Lett. **B79**, 109 (1978).

[43] A. F. Falk, M. Luke and M. J. Savage, Phys. Rev. **D53**, 6316 (1996).

[44] S. Brodsky, G.P. Lepage and P. Mackenzie, Phys. Rev. **D28**, 228 (1983).

[45] M. Gremm and I. Stewart, Phys. Rev. **D55**, 1226 (1997).

[46] A.F. Falk and M. Luke, Phys. Rev. **D57**, 424 (1998).

[47] I. I. Bigi, M. Shifman, N.G. Uraltsev and A. Vainshtein, Phys. Rev. **D52**, 196 (1995).

[48] T. Mannel, Phys. Rev. **D50**, 428 (1994).

[49] M. Gremm and A. Kapustin, Phys. Rev. **D55**, 6924 (1997).

[50] A. Kapustin and Z. Ligeti, Phys. Lett. **B355**, 318 (1995).

[51] C. Bauer, preprint UTPT-97-19, hep-ph/9710513.

[52] A. Ali and C. Greub, Z. Phys. **C49**, 431 (1991); Phys. Lett. **B259**, 182 (1991).

[53] M.S. Alam et al. (CLEO Collaboration), Phys. Rev. Lett. **74**, 2885 (1995).

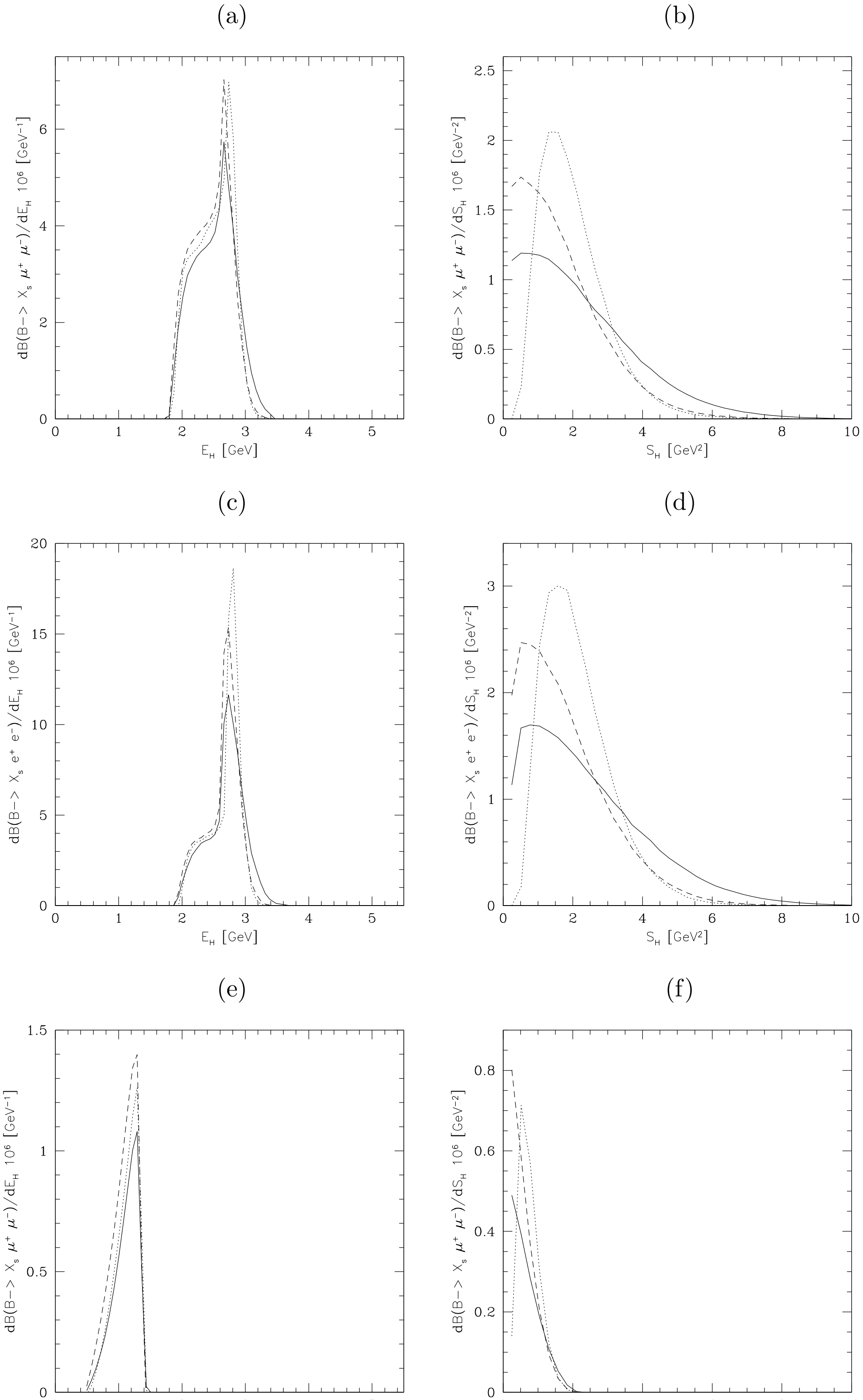

Figure 10: *Hadron spectra in* $B \to X_s \ell^+ \ell^-$ *in the Fermi motion model with the cuts on the dilpeton mass defined in eq. (78); (a),(c),(e) for the hadronic energy and (b),(d),(f) for the hadronic invariant mass corresponding to cut A,B,C, respectively. The solid, dotted, dashed curves correspond to the parameters* $(\lambda_1, \bar{\Lambda}) = (-0.3, 0.5), (-0.1, 0.4), (-0.15, 0.35)$ *in (GeV*^{2}*, GeV), respectively.*